CONSTRUCTION OF A COLLAGEN-BASED, SPLIT THICKNESS CORNEA SUBSTITUTE

A THESIS SUBMITTED TO
THE GRADUATE SCHOOL OF NATURAL AND APPLIED SCIENCES
OF
MIDDLE EAST TECHNICAL UNIVERSITY

BY

AYLIN ACUN

IN PARTIAL FULFILLMENT OF THE REQUIREMENTS
FOR
THE DEGREE OF MASTER OF SCIENCE
IN
BIOTECHNOLOGY

JANUARY 2013

Approval of the thesis:

CONSTRUCTION OF A COLLAGEN-BASED, SPLIT THICKNESS CORNEA SUBSTITUTE

submitted by **AYLIN ACUN** in partial fulfillment of the requirements for the degree of **Master of Science in Biotechnology Department, Middle East Technical University** by,

Prof. Dr. Canan Özgen
Dean, Graduate School of **Natural and Applied Sciences**

Prof. Dr. Gülay Özcengiz
Head of Department, **Biotechnology**

Prof. Dr. Vasıf Hasırcı
Supervisor, **Biological Sciences Dept., METU**

Prof. Dr. Kuyaş Buğra
Co-Supervisor, **Dept. of Mol. Biol. and Gen., BOUN**

Examining Committee Members:

Prof. Dr. Nuhan Puralı
Biophysics Dept., Fac. Med., Hacettepe University

Prof. Dr. Vasıf Hasırcı
Biological Sciences Dept., METU

Assoc. Prof. Dr. Ayşen Tezcaner
Engineering Sciences Dept., METU

Assoc. Prof. Dr. Mayda Gürsel
Biological Sciences Dept., METU

Assoc. Prof. Dr. Çağdaş Son
Biological Sciences Dept., METU

Date: 17.01.2013

ii

I hereby declare that all information in this document has been obtained and presented in accordance with academic rules and ethical conduct. I also declare that, as required by these rules and conduct, I have fully cited and referenced all material and results that are not original to this work.

Name, Last Name: Aylin Acun

Signature   :

ABSTRACT

CONSTRUCTION OF A COLLAGEN-BASED, SPLIT THICKNESS CORNEA SUBSTITUTE
Acun, Aylin
M.Sc., Department of Biotechnology
Supervisor: Prof. Dr. Vasıf Hasırcı
Co-Supervisor: Prof. Dr. Kuyaş Buğra
January 2013, 62 pages

Cornea is the transparent outermost layer of the eye. It is a thin (500 μm) multilayer tissue which performes around 75% of the total refraction in the eye. It also protects the inner layers against any type of damage. Since it is avascular, the three cellular layers of cornea always need transport of nutrients and other materials in and out of the tissue via diffusion. Any change in shape, transparency or thickness of cornea, or physical damages and infections, may cause serious defects. The conventional methods are satisfactory in the treatment of mild injuries but severe cases require the substitution of the tissue with an equivalent. Keratoprosthesis and donor corneas that are used as replacements do not completely meet requirements.

Tissue engineering can be an alternative method for preparing a biocompatible and stable cornea equivalent. The ability to choose from a variety of materials and the ability to incorporate bioactive agents allow the researchers to tailor make the construct. The structure needs to be seeded with the patient's own cells and cultured *in vitro* to yield an optimal corneal replacement.

In this study a novel, split thickness cornea replacement is proposed to substitute the two upper cellular layers (epithelium and stroma) of the native cornea. The design includes a chondroitin sulfate impregnated collagen type I (isolated from rat tail) foam (CSXLF) produced by lyophilization carrying electrospun fibers of the same polymer collected directly on top of the foam, forming the bilayer structure (Fo-Fi). The fiber layer was intended to separate the epithelium and the stroma of the reconstructed cornea yet to allow material transfer in between. The foam layer (bottom) was crosslinked by N-ethyl-N-[3-dimethylaminopropyl] carbodiimide (EDC), and *N*-hydroxy succinimide and after fiber deposition the bilayer was further stabilized with physical crosslinking (DHT method).

The physical characterization of the foam showed that their pore sizes (10-200 μm) and porosities (around 70%) were well within the desired range for typical tissue engineering applications. The cell free wet thicknesses of both single and bilayer constructs were close to that of the native stroma and light transmittance through these scaffolds was quite high (around 82% in the 500-700 nm range). The scaffolds were also tested for their stability and shown to be suitable for *in vitro* testing.

In vitro studies were performed using retinal pigment epithelial cells (RPE, D407 cell line) and isolated human corneal keratocytes (HK) to reconstruct the epithelium and the stroma, respectively. Three types of constructs were prepared; only HK seeded Fo-Fi constructs, RPE-HK seeded CSXLFs, and RPE-HK seeded Fo-Fi constructs. All were shown to support cell attachment and promoted cell proliferation as was shown by the cells that covered the inner and outer spaces of the scaffolds. The fiber layer prevented the mixing of the two cell types, without hindering material exchange between them. Moreover, when co-cultured for 14 days, the keratocytes started to deposit collagen type I, a specific marker of these cells. In contrast, ECM deposition could not be observed in the single type cell seeded samples. The co-cultured bilayer construct was tested for suturability at the end of 31 days of *in vitro* incubation and it was shown that it could be successfully sutured without any major tears. Under the light of these results it was concluded that both the single layer and the bilayer constructs show promise for use as split thickness cornea replacements.

KEYWORDS: Cornea, Tissue Engineering, Split Thickness, Transmittance, Suturability.

ÖZ

KOLLAJEN TEMELLİ, YARI KALINLIKLI YAPAY KORNEA YAPIMI

Acun, Aylin
Yüksek Lisans, Biyoteknoloji Bölümü
Tez Yöneticisi: Prof. Dr. Vasıf Hasırcı
Ortak Tez Yöneticisi: Prof. Dr. Kuyaş Buğra
Ocak 2013, 62 sayfa

Kornea gözün en dış katmanını oluşturan ince ve şeffaf bir dokudur. İnce olmasına rağmen bir kaç katmandan oluşur ve gözün ışık kırma ve odaklama kapasitesinin %75'i kornea tarafından sağlanır. En dış katman olduğundan gözün iç kısımlarını koruyucu bir görevi de vardır. Kornea damarsız bir yapıdır ve besin, oksijen gibi maddelerin alınması ve/veya atık maddelerin uzaklaştırılması için dokuyu oluşturan 3 hücreli katman arasında difüzyonla gerçekleştirilen bir madde alışverişi vardır. Korneanın şeffaflığı, şekli veya kalınlığındaki değişikler ile enfeksiyon ya da darbeler dokunun işlevini kaybetmesine sebep olabilir. Özellikle ileri derece travmalar dokunun uygun bir eşleniğiyle değiştirilmesini gerektirir. Günümüzde bu, bağışlanan korneanın veya yapay korneanın (keratoprotez) hasta dokuyla değiştirilmesi şeklinde yapılmaktadır fakat iki yöntemin de önemli dezavantajları bulunmaktadır.

Doku mühendisliği ile üretilecek yapay dokuların kullanımı alternatif bir yöntem olarak görülmektedir. Bu yöntemle değişik biyomalzemeler ve metotlar kullanılarak istenilen güç ve özelliklerde yapılar üretilebilmekte ve biyoaktif moleküllerin eklenmesiyle doku oluşumu yönlendirilebilmektedir. Oluşturulan yapıların hastanın kendisinden alınan hücrelerle ekilmesiyle de, nakil edilen dokuların aksine, hastanın bağışıklık sistemini uyarmayacak bir doku eşleniği oluşturulması öngörülmektedir.

Bu çalışmada doğal korneanın üst iki katmanını (stroma ve epitelyum) taklit eden yarı kalınlıklı bir yapı tasarlanmıştır. Bu yapı kondroitin sülfata batırılmış kollajen tip 1 bazlı sünger bir matrisin üzerine aynı polimerden elektro eğirme yöntemiyle üretilmiş fiberlerin toplanmasıyla oluşturulmuştur. Yapının sünger katmanı (alt) kimyasal yöntemlerle, fiber katmanı (üst) ise fiziksel yöntemlerle çapraz bağlanarak sağlamlaştırılmıştır. Yapıdaki fiber katman epitelyum ve stroma hücrelerini aralarındaki madde transferini etkilemeyecek şekilde birbirinden ayırmak amacıyla eklenmiştir.

Yapının fiziksel özellikleri incelenmiş ve sünger katmanın gözenekliliği ve gözenek boyutlarının doku mühendisliği uygulamaları için uygun olduğu görülmüştür. Ayrıca hücresiz, ıslatılmış örneklerin doğal korneanın stroma katmanı kalınlığına yakın bir kalınlıkta oldukları ve ışık geçirgenliklerinin yüksek olduğu belirlenmiştir. Yapıların dayanıklılıklarının da istenen seviyede olduğu görülmüş ve bunların hücre kültürü çalışmalarına uygun olduğuna karar verilmiştir.

Hücreli çalışmalarda insan kornea keratositleri (HK) ve retinal pigment epitelyum (RPE) hücreleri, ko-kültür tekniğiyle korneanın stroma ve epitelyum katmanlarını oluşturmak üzere kullanılmıştır. Üç farklı tip iskele hazırlanmıştır: sadece keratosit ekili ve ko-kültür uygulanmış tek katmanlı ve ko-kültür uygulanmış iki katmanlı (sadece sünger). Bütün örneklerde hücre tutunması ve çoğalması gözlenmiştir. 14 günlük kültür sonunda ko-kültür uygulanmış örneklerde keratositlerin kendilerine özgü olan kollajen tip 1 salgıladıkları fakat tek başlarına kültür edildiklerinde salgılamadıkları görülmüştür. 31 günlük inkübasyon sonunda ko-kültür uygulanan iki katmanlı örneğin dikilebilirliği sınanmış ve örneğin büyük yırtıklar oluşmadan dikilebildiği gözlemlenmiştir.

Bütün sonuçlar ışığında hazırlanan tek veya iki katmanlı yapıların kornea doku mühendisliği uygulamaları için uygun olduğu çıkarımı yapılmıştır.

Anahtar Kelimeler: Kornea, Doku Mühendisliği, Yarı Kalınlık, Işık Geçirgenliği, Dikilebilirlik.

Dedicated to my family

ACKNOWLEDGEMENTS

TABLE OF CONTENTS

LIST OF TABLES

TABLES

LIST OF FIGURES

FIGURES

LIST OF ABBREVIATIONS

3D	Three Dimensional
BSA	Bovine Serum Albumin
b-FGF	Basic Fibroblast Growth Factor
cm	Centimeter
CO_2	Carbon Dioxide
CS	Chondroitin Sulfate A
CSLM	Confocal Laser Scanning Microscopy
CSXLF	Chondroitin Sulfate Impregnated Foam
d	days
DAPI	4', 6-Diamidino-2-Phenylindole
DHT	Dehydrothermal Treatment
DMEM	Dulbecco's Modified Eagle Medium
DMEM/F12	Dulbecco's Modified Eagle Medium/Ham's F12 Nutrient Mixture
DMF	Dimethylformamide
DMSO	Dimethyl Sulfoxide
ECM	Extracellular Matrix
EDC	N-Ethyl-N-[3-Dimethylaminopropyl]Carbodiimide
FBS	Fetal Bovine Serum
FITC	Fluorescein Isothiocyanate
Fo-Fi	Foam-Fiber Scaffold
g	gram
GAG	Glucosaminoglycan
h	hour
HAc	Acetic Acid
HFIP	1,1,1,3,3,3-Hexafluoroisopropanol
min	minute
mm	millimeter
NaCl	Sodium Chloride
NHS	N-Hydroxysuccinimide
PBS	Phosphate Buffer Saline
PCL	Poly(E-Caprolactone)
PEG	Polyethylene Glycol
PEGDA	Polyethylene Glycol Diacrylate
Pen/Strep	Penicillin/Streptomycin
PGA	Poly(glycolic acid)
PHB	Poly(3-hydroxybutyrate)
PHBV	Poly(3-hydroxybutyrate-co-3-hydroxyvalerate)
PHEMA	Poly(2-hydroxyethyl methacrylate)
PLGA	Poly(lactic acid-co-glycolic cid)
PLA	Poly(lactic Acid)
PMMA	Poly(methyl methacrylate)
PVA	Poly(vinyl alcohol)
SDS-PAGE	Sodium Dodecyl Sulfate- Polyacrylamide Gel Electrophoresis
SEM	Scanning Electron Microscopy
XLF	Crosslinked Foam

<div align="center">

CHAPTER 1

INTRODUCTION

</div>

1.1. Cornea

1.1.1. Anatomy of Cornea

1.1.1.1. Macrostructure of Cornea

Cornea is the outermost layer of the eye. It is a transparent and an avascular tissue. The curved shape of cornea, along with its transparency, contributes to its refractive function in the eye [1]. Up to 78 % of cornea is water and this specific level of hydration is another important feature of cornea to function as an optical element [2].

Since cornea is an avascular tissue, it depends on diffusion for material transport in and out. Aqueous humor, which is located right underneath the cornea, is responsible for the transport of required growth factors and nutrients. Tear is the second route and the sole source of O_2 for the cornea. The waste products and CO_2 are also removed via diffusion as well [3].

The cornea is a thin tissue, approximately 500 μm thick in the center [4], 750 μm to 1000 μm at the periphery [4, 5] and constitutes only one-sixth of the total thickness of the eye (Figure 1.1).
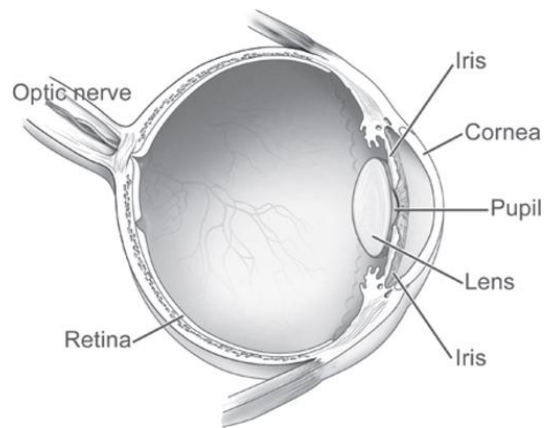
Figure 1. 1. Anatomy of the eye [3].

The maintenance of the thickness of the cornea is crucial for its refractive powers, and therefore, for proper vision. Its stability is a result of a series of cell junctions and pumps which control the water – ion ratio, and thus the swelling [3].

Cornea has a spherical shape, yet it is not a perfect sphere. A normal human cornea is about 12 mm in diameter and has a curvature radius of 7.8 mm at the central anterior region [3].

Cornea is in contact with several other tissues like conjunctiva, tear film, eyelids, and commensal organisms of the conjunctival sac (Coster *et al.,* 2002). The optical nerve endings at conjunctiva lead to the closure of the eyelid even with the smallest contact with the cornea [6].

1.1.1.2. Microstructure of Cornea

Cornea is composed of 5 distinct layers. Three of these layers are cellular and the other two are membranous. The layers from inside towards outside are endothelium, stroma and epithelium. The 3 layers are separated from each other by means of Bowman's membrane and Descemet's membrane (Figure 1.2.).
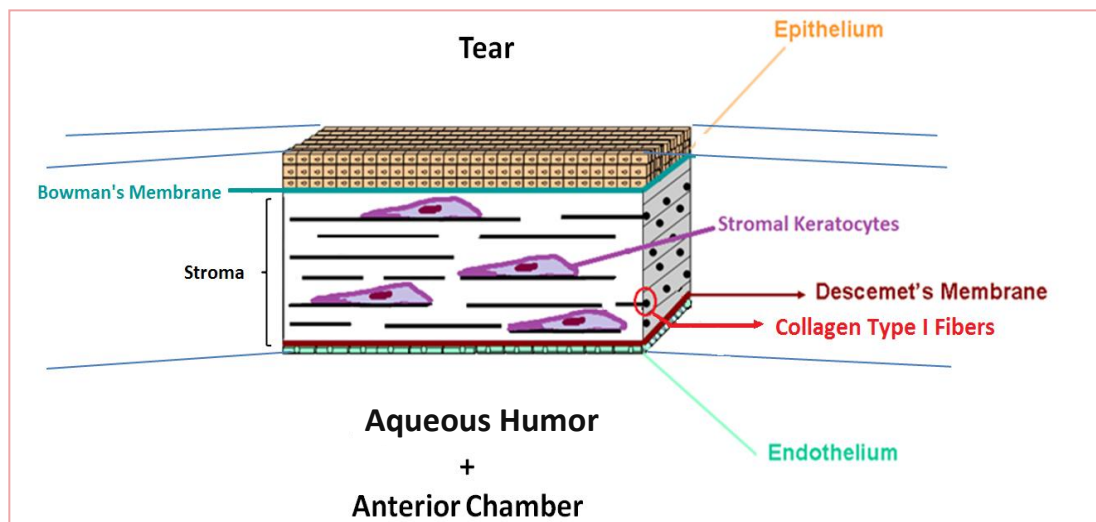
Figure 1. 2. Microstructure of cornea

Epithelium, the outermost layer of the cornea, is composed of a stratified epithelial cell layer. It makes up approximately the 10 % of total thickness of the cornea [3]. Five to 7 layers of corneal epithelial cells are present in a normal human cornea. The uppermost layer of epithelium is composed of superficial cells, underneath lies the wing cells while basal cells comprise the bottom layer [7]. The basal columnar cells are the only cells that are capable of mitosis. The upper layers are composed of the resulting daughter cells.

Any physical damage or foreign material from outside will be met by the epithelium, which has a protective role. Strengthened by the tight junctions between the epithelial cells, epithelium can act as a physical barrier, preventing the penetration of any foreign material or microorganisms. The cell to cell junctions enable the epithelium to endure shear forces resulting from blinking and eye movement, making the epithelium a mechanical barrier as well.

As the outermost layer, epithelium is in direct contact with tear. It must successfully transport O_2, nutrients and growth factors to the inner compartments via diffusion. Moreover, epithelium is responsible for keeping the water-ion balance of the cornea. As a result of specialized cell to cell junctions, epithelial cells are strongly connected to each other. This allows them to prevent excess water and ion diffusion to the inner layers, preventing the swelling of stroma [2].

Bowman's membrane, an interwoven fiber mesh of collagen type I fibers with pores, (Abrams *et al*, 2000) separates the epithelium and the stroma. As an acellular layer, the main role of Bowman's membrane is protection of the underlying layers [6]. As the studies of Nagy *et al.* have shown, sensitivity against UV light is higher in eyes without the epithelial layer and Bowman's membrane than eyes with removed stromal layers [8]. In another study it was shown that the Bowman's layer along with the epithelium is more effective than the posterior layers in UV-B (280–330 nm) absorption by cornea [9].

Stroma is the second cellular and the thickest layer of the cornea. It makes up approximately 90% of the total thickness of cornea [2]. The cells occupying this layer are stromal keratocytes, which are

fibroblast-like cells that adhere to each other via cell-to-cell junctions [2]. This layer is mainly composed of the extracellular matrix (ECM) produced by the keratocytes. The main components of the ECM are collagens type I, V, VI and XII, and glycosaminoglycans decorin, keratocan, lumican and mimecan [2, 10]. The most abundant protein in corneal stroma is collagen type I and its fibers are highly arranged. This arrangement is in the form of lamellae, neighboring ones being orthogonal (90°) to each other (Figure 1.3) [10-13].

Figure 1. 3. Collagen type I lamellae oriented perpendicular to each other [14].

Stroma is composed approximately of 300 lamellae at the center and up to 500 lamellae at the periphery, the limbus. This anisotropic nature of the stroma is the reason that it and the whole cornea are transparent [3]. The relationship of transparency and fiber arrangement in cornea was explained by Maurice (1957). He suggested that the collagen fibers do not cause light scatter when they are arranged in lamellae orthogonal to each other as much as they would if they were randomly distributed. He also mentioned that in addition to the special arrangement, small diameter of collagen fibers also contribute to the transparency of the cornea.

The second important component of the stroma are proteoglycans. Sulfated glycosaminoglycans, such as chondroitin sulfate and keratin sulfate, found in the structure of decorin and lumican, help keep stroma moist by retaining water [2, 11]. In addition, proteoglycans present in the stroma are responsible for the preservation of the spacing between the collagen lamellae [2].

The second acellular and the fourth layer of the cornea is Descemet's membrane. Similar to Bowman's membrane, Descemet's membrane is composed of interwoven collagen fibers with pores between them. Although the fiber diameters of the two membranes are both in the nanometer range, Descemet's membrane is packed more densely than Bowman's membrane [12]. Therefore, Descemet's membrane is tough and protects the endothelium. However, being densely packed does not prevent the material transfer from the aqueous humor to the stroma [13].

Endothelium is the bottom layer of cornea consists of monolayer of endothelial cells and serves two major functions. The first one is to prevent excess water uptake into the stroma. Endothelial cells achieve this via their cell-to-cell junctions acting as a physical barrier and by the action of the sodium/potassium and ATPase pumps. With these two routes endothelium either physically restricts the water flow from aqueous humor to the stroma or it pumps back the excess water coming from the aqueous humor, acting as a biological pump [1, 3, 13]. It is very important that the stroma remains rather dehydrated because when it absorbs water due to its highly hydrophilic nature, the organization of lamellae and the transparency and the refractive index of the cornea are affected [2].

1.1.2. Functions of Cornea

Cornea has two vital functions: optical and protective. Cornea is a critical optical element that provides the 75% of the total refractive power in the eye. The highly organized collagen lamellae, the well maintained thickness and hydration level keeps the cornea transparent. The slightest difference in the transparency or the thickness of cornea would lead to visual problems [2, 15].

The second important function of cornea is protection. Cornea protects the inner layers not only by serving as a physical barrier, but also by absorbing UV-B and enduring the stress created by inner pressure of aqueous humor and movement of the eye [3]. Cornea serves as a physical barrier and prevents internalization of any impurity as a result of the action of strong cell-to-cell junctions in the epithelium [2].

Cornea is an elastic tissue, and can endure the internal pressure of the aqueous humor, and its special fibril arrangement provides sufficient mechanical strength to handle the tensile stress created by the eye movement [2]. The protective role of cornea is enhanced by its sensitive nerve endings which cause the closure of eye lid even with the smallest contact with the cornea [6]. Moreover, the high regenerative capacity of epithelium decreases the probability of internal damage [15, 16].

1.1.3. Pathology of Cornea

Cornea is susceptible to all kinds of contacts with external sources. Despite its superior mechanical properties, high regenerative capacity and durable structure, cornea can be severely damaged as a result of impacts, infections or physiological conditions, and inherited corneal dystrophies it loses its transparency, shape or any other characteristics.

External thermal, mechanical or chemical impacts can cause severe corneal damage and even blindness [17]. Chemical spills, especially alkali burns, cause immediate loss of vision. Acid burns cause the proteins to coagulate and this prevents deeper penetration. Alkali burns cause changes in the structure of collagen and glycosaminoglycans causing corneal ulceration, scarring or even permanent loss of vision [18].

Corneal edema is a pathological case which is caused by the excessive water uptake by the epithelium or stroma [15]. Vascularization of cornea may result from surgical operations or infectious diseases and this critically affects transparency. Presence of blood vessels and/or lymphatic vessels in the cornea is the second most common cause of corneal blindness [19].

Corneal infections like keratitis, can be the result of scarring, microbial infections or from the use of contact lenses. The study of Chalupa presents evidence that extended contact lens use causes severe microbial keratitis [20]. A common infectious disease of the cornea called trachoma occurs due to infection by the bacteria *Chlamydia trachomatis*, which causes corneal ulceration and scarring and even corneal blindness if not treated [15, 17].

There are several types of corneal dystrophies and Fuch's dystrophy is one of the most common. It is an endothelial dystrophy and leads to the thickening of stroma due to excessive hydration [15, 21]. Reis-Buckler's dystrophy causes the replacement of Bowman's membrane with a fibrovascular material and ends up in the epithelial erosion and corneal scarring. Other dystrophies like lattice dystrophy, macular dystrophy, keratoconus and anterior membrane dystrophy are mostly bilateral and cause impaired vision or even corneal blindness by disturbing the transparency or disrupting the organization of the cornea [15].

1.1.4. Current Treatments Available for Corneal Diseases and Dystrophies

Several different clinical therapies against mild to severe corneal damages are available. In mild epithelial degeneration and dehydration problems, treatment can be done via application of pharmacological agents [22]. One example to such applications is autologous serum application. The

degeneration in epithelium is retarded by the action of vitamins and growth factors present in the serum [19]. Similarly the mild infections can be overcome by the administration of antibiotics, and corneal inflammations can be reduced by the application of anti-inflammatory agents [15].

Another approach towards the treatment of corneal diseases and dystrophies is gene therapy. With this method it is aimed to remove the cause of the disease rather than to simply suppress the symptoms. It is applied to a wide variety of diseases like corneal scarring, corneal vascularization and inflammation [22].

These treatment methods, however, are only applicable in cases where the cornea damage is mild. More severe cases require different methods of treatment or replacement of the damaged site or the whole cornea. Penetrating keratoplasty or cornea transplantation is preferred when the cornea is irreparably damaged. In this operation, the degenerated cornea is replaced by a healthy cornea from a donor. For this operation to be successful, the donated tissue should be compatible with that of recipient. As the cornea is a non-vascularized tissue, there is a greater chance to find a suitable replacement [23].

Instead of transplanting a donated tissue, artificial corneas may be used. The procedure of replacing the cornea with its artificial equivalent is called prostho-keratoplasty, and the artificial corneas are named keratoprostheses [18]. The idea of using keratoprostheses has begun in the 1800s with the use of hard materials like glass or quartz. In following years the design was modified to introduce a skirt. The design with a transparent optical core and a porous skirt keratoprostheses. The core transparent and with the desired curvature, fulfills the optical requirements of cornea, whereas the porous skirt helps anchor the core to the eye by cell growth into the pores [1, 18].

Over time the material choice changed and more biocompatible synthetic polymers started to be used. The first synthetic polymer to be used as an artificial cornea material was poly(methyl methacrylate) (PMMA) [18]. The trials with PMMA were succeeded with those with other synthetic polymers like poly(2-hydroxyethyl methacrylate) (PHEMA), silicone rubber and polyurethane. Another approach was the use of skirts made of dental or bone tissue derived from the patient attached to a PMMA core, forming a structure called osteo-odonto keratoprostheses (OOKP). Two examples of core-skirt keratoprostheses in clinical use are the Boston keratoprostheses and AlphaCor keratoprostheses [1].

1.1.5. Need for Corneal Tissue Engineering

All of the remedies mentioned above have some limitations or drawbacks. For example, pharmacological agents are not successful in severe corneal damages. They may only help to relieve the symptoms.

Similarly, gene therapy seems very promising as a treatment method, however, it is not yet accessible in all parts of the world and its application is limited to patients suffering from common corneal problems; therapies aiming to cure specific inherited dystrophies are yet to be designed [22].

In severe cases, replacement of the cornea with a natural or an artificial substitute is required. The most common method to treat severe cases of genetic, physiological or physical origin is penetrating keratoplasty. However, there are many limitations and risks of this procedure [1, 15, 18]. Firstly, the donor tissue and the tissue of the recipient should be compatible to prevent rejection. Secondly, transplantation of an allogenic tissue carries the risk of donor-derived infection. Surgical complications like hemorrhage and damage to underlying structures as well as postoperative complications such as graft failure, graft rejection and astigmatism are important risks [15]. Finally, and most importantly, for a transplantation procedure there is the donor scarcity issue. The availability of donor corneas further decreases as the application of laser *in situ* keratomileusis (LASIK), a corrective procedure makes corneas unsuitable for transplantation. With all these limitations, the chance of finding a suitable donor cornea is very low [1].

According to a survey conducted in Sweden, in the two years after transplantation the rejection rate was around 15% [24]. This rate increased with time, reaching 45% rejection at 10 to 15 years following the operation [1]. Moreover, occurrence of specific conditions like vascularization, severe dehydration of cornea and alkali burns or dystrophies like Stevens-Johnson syndrome decreased significantly the success of transplantation [2].

The second most common clinical application used to overcome the drawbacks of transplantation is the use of artificial cornea (keratoprostheses). Keratoprostheses have some disadvantages too; they can be extruded, cause inflammation, infection, epithelial downgrowth or glaucoma [18]. In a study about the long term use of keratoprostheses, it was observed that the success rate decreases with time because the complications listed above increase in frequency [25]. They, however, are not yet perfect and developments in this field include the use of tissue engineering and regenerative medicine to produce artificial corneas.

When all current therapies are considered, there appears to be no satisfactory corneal replacement method. That is why tissue engineering currently draws much attention.

1.2. Tissue Engineering

Tissue engineering is defined as a multidisciplinary field that brings the basic sciences and engineering principles together [26] with the aim of improving, repairing or replacing a damaged, malfunctioning or diseased tissue with a healthy, artificial equivalent [27].

Tissue engineering studies have begun to emerge in the early 1990s and it continues to attract attention of scientists and public [28]. Artificial substitutes for a wide variety of tissues, such as skin, nerve, cardiac muscle, cornea, blood vessel, cartilage and bone, have been successfully prepared in the lab scale studies by tissue engineering [26, 27]. The engineering of tissues with significantly different characteristics is being attempted by mimicking the unique biological, physical and chemical properties of natural equivalents [27].

The most common way to construct a substitute tissue is to use cells which are supported by a scaffolding material loaded with specific biological factors to improve its function as an artificial tissue [26]. One of the three main components of a tissue engineered construct, cells, are first acquired from a specific source (preferably in the patient's own body) and grown in a suitable culture environment to achieve the required number of cells to construct a tissue replacement. The second component, the biomaterial or the scaffold, is prepared in a special manner to fulfill the function of the tissue of interest. In order to improve the interaction between cells and the scaffold and to guide cells during differentiation, a third component, growth factors, are integrated into the structure. Next, the proliferated cells are seeded onto the scaffold which is then incubated in its specific culture media for the construct to mature and serve as a full functioning tissue equivalent (Figure 1.4.) [29].
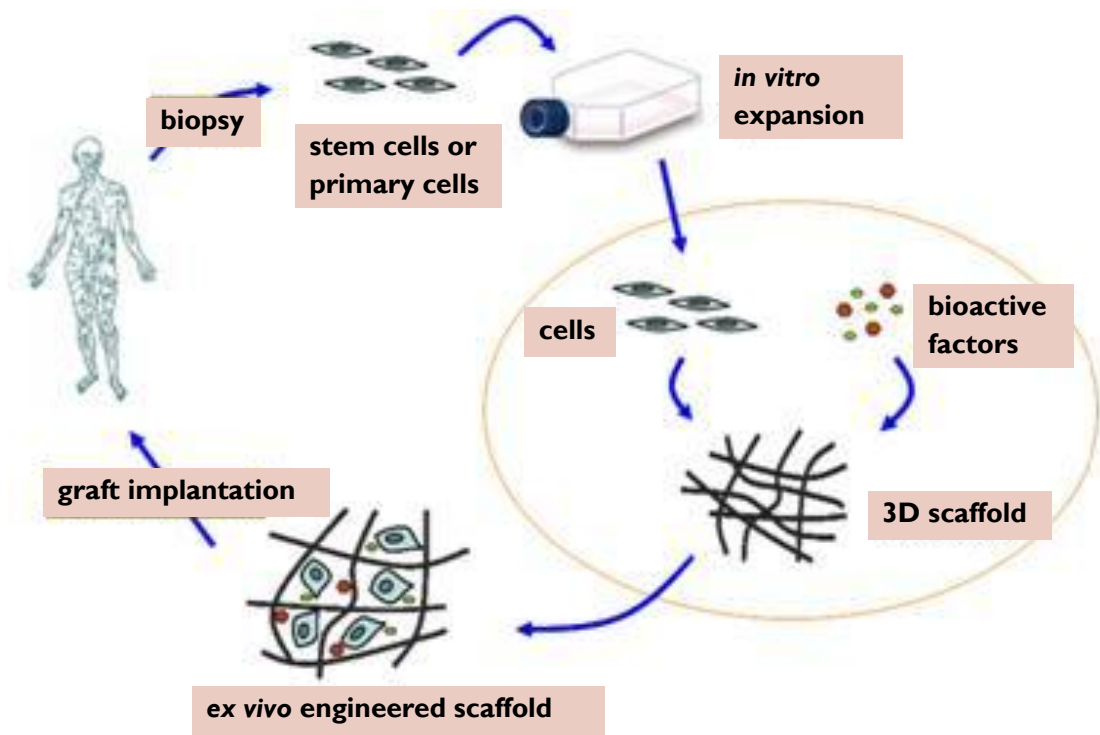
Figure 1. 4. Tissue engineering strategy [30].

1.3. Cell Sources in Tissue Engineering

Cell sources used in tissue engineering can be grouped according to their differentiation state as i) embryonic stem cells, ii) adult stem cells and iii) fully differentiated cells. After isolation of cells from a biopsy from any tissue, the fully differentiated cells of that tissue are obtained. These cells then need to be grown to obtain the required number sufficient to construct a fully functioning tissue. This culture of the isolated cells is called the primary culture. Extensive proliferation of these cells is not desired because there is the risk of dedifferentiation. Dedifferentiated cells lose their characteristic properties like production of tissue specific extracellular matrix or their phenotypic markers [31-34]. Although isolated cells may undergo dedifferentiation, their use is very common in the engineering of many different tissues like bone, skin, cardiac muscle, cartilage and cornea [35-39].

Use of cells isolated from a tissue is not applicable for all kinds of tissues such as hard to reach tissues like nerves in the spinal cord, In these cases a cell source different than the target tissue is needed. The other common cell source is stem cells, which are undifferentiated cells that have the potential to differentiate into more than one type of cell [34].

Embryonic stem cells are stem cells that are immortal and they have pluripotency, which means that they can form any type of cell in the body [26]. These cells are harvested from embryos at their early developmental stages and are discarded because they are not suitable for *in vitro* fertilization studies,. They are easy to isolate and they can proliferate fast without undergoing differentiation.

Adult stem cells are not capable of differentiating into every cell type found in the body but still they can form more than one type of cell which are closely related to the tissue they originate from. For example, bone marrow stem cells can be differentiated into bone, cartilage, tendon, ligament cells as well as into hepatocytes and heart muscle cells [40]. Despite these appealing properties of stem cells, they also have some limitations. Since they need to be differentiated into a desired cell type, the induction of differentiation should be highly controlled to avoid tumor formation because of the tumorogenic nature of stem cells [34].

1.3.1.   Cells Types Used in Cornea Tissue Engineering

A wide range of cell types can be used to prepare a full or split thickness corneal construct, comprising one or two layers of the tissue. Mainly the cells isolated from the respective layers of the cornea are used in the construction. Isolated human corneal epithelial cells and limbal corneal epithelial cells are used in the reconstruction of the epithelial layer [39, 41-43], use of immortalized cell lines of corneal epithelial cells were also reported [44-46], as well as the use of limbal stem cells [39]. For the construction of the stroma, different cell types like isolated primary stromal cells [43, 45, 47, 48], precursor cells or cell lines [44, 49, 50], or dermal fibroblasts [48, 51] were seeded on to the scaffolds. Similarly, endothelium of corneal constructs was populated by isolated cells [43] or immortalized endothelial cell lines [39, 44, 45].

1.3.2.   The Co-Culture

Tissue engineering simply aims the preparation of constructs that closely mimic the natural tissues. As many tissues are composed of more than one cell type, including all required cell types in a 3D construct is a necessity because each cell type has a specific function and cell to cell and cell to ECM interactions play a critical role in the function of a tissue. In order to successfully produce a multilayered tissue equivalent as many as two or three different cell types need to be seeded and grown on a scaffold in a co-culture.

Co-cultures have been extensively used in the construction of several tissues like cornea, heart valve, urethra wall, cartilage, skin [39, 52-56]. Mostly the co-culture is initiated by seeding and incubating one cell type for a while, and then the second cell type to the respective site on the scaffold. If there is a third cell type then it is seeded following attachment of the second cell type.

Vascularization of a construct is also achieved by the addition of vascular epithelial cells needed for the vessel formation, to the construct already seeded with the main cell type(s) [54].
The third use of the co-culture method is to provide a cell layer to support the other. A feeder layer may support the proliferation and proper function of the cells [57, 58] or provide differentiation factors to the other cell layer [59].

1.4.   Scaffold Types Used in Tissue Engineering

Throughout the history of tissue engineering tissues possessing extensively different characteristics were engineered successfully. The different characteristics, however, were not brought solely by the functions of the cells seeded onto the scaffolds. The differences in scaffold structure have also contributed significantly in the preparation of a fully functioning tissue equivalent. Mostly common tissue engineering scaffold types (or forms) are foams, films, patterned films, fiber meshes, and membranes. In addition, decellularized tissues are used as substrates for tissue engineering applications.

The differences between the scaffolds are caused by two important choices: the fabrication technique and the material.

1.4.1.   Scaffold Fabrication Techniques

Tissue engineering scaffolds have some common requirements to fulfill. A tissue engineering scaffold should preferably be (i) biodegradable in a controllable manner and with no harmful degradation products (ii) match the growth of the surrounding tissue so that the natural tissue can replace the artificial equivalent. (iii) the scaffolds should accommodate cells and have room for proliferation and for the ECM they will produce. For this, they need to be highly porous. (iv) They should have pore interconnectivity since material transfer in and out of the construct is essential for the cells to be viable. (v) Mechanical properties of a scaffold should match that of a specific to tissue to be constructed [60].

Freeze Drying: One of the most commonly used methods is freeze drying, which yields highly porous foams or sponges. In this method, polymer is dissolved in its solvent. Then it is frozen while preserving the thickness of the solution. Finally by drying under vacuum in frozen state the solvent is sublimed, leaving pores at its previous positions. Since the polymer solution was homogeneous, the pores created by solvent crystals are interconnected, and the resulting structure is highly porous but pore sizes are not uniform.

Electrospinning: Another technique used is electrospinning, by which nano-micro scale fibers are produced. This method utilizes a syringe pump to expel the polymer solution through the high voltage applied syringe nozzle. As the polymer solution leaves the nozzle tip, it forms a jet of polymer by the effect of applied potential. This polymer jet is directed to a grounded collector, placed at a defined distance from the needle tip. The solvent evaporates until the polymer jet reaches the collector resulting in thin polymer fibers accumulated on the collector. The orientation of the fibers and the shape of the construct as a whole can be changed with the choice of collector. Furthermore, the diameter and structure of the fibers are dependent on several parameters like the distance between the collector and needle tip, polymer ejection rate, voltage applied, diameter of the nozzle, solvent type and polymer concentration.

Solvent Casting/Particulate Leaching: Solvent casting/particulate leaching is another technique that yields highly porous foams. A porogen is added to the polymer solution and is leached after the drying of the polymer. A material that will dissolve in non-solvent of the polymer is used as a porogen. The leaching of the porogen is achieved by simply dissolving it in its solvent. As a result the remaining polymer structure has a high number of interconnected pores left behind by the porogen. This method is preferred since pore sizes can be controlled by the choice of porogen, and its size and amount.

Fiber Bonding: Fiber bonding, another method for scaffold fabrication, is one of the simplest methods. The nonwoven fiber meshes are made and then exposed to heat just above their melting point so that the polymer fibers fuse at the intersection points and these results in a highly porous network. Although easy to perform, this method is not applicable to all polymers and the scaffold fabricated may not be mechanically strong.

Melt Molding: Another technique used in scaffold fabrication is melt molding. This method is similar to solvent casting/particulate leaching method since the pores are generated by leaching out a porogen. The difference lies in the molding process, which is done via exposure to high heat. The molded polymer-porogen mixture is cooled down and the porogen is leached out leaving pores behind, however, the scaffold has the exact shape of the mold.

Membrane Lamination: A 3D scaffold can be generated using 2D porous membranes or films by lamination. In this method several layers are laminated to comprise a 3D structure. The layers are joined by the application of a solvent or heat or a glue to the interfacial surface. The shape and thickness of the scaffold can be controlled but the interconnectivity might be limited.

Phase Separation: Phase separation is another method for the production of highly porous scaffolds. The polymer and the solvent are separated by cooling the homogeneous polymer mixture below the freezing point of the solvent. In this way two phases, solvent and polymer, are formed, and the solvent portion is then removed by sublimation following the freezing step. Remaining is the porous polymer structure, in which bioactive molecules can be incorporated.

Rapid Prototyping: Rapid prototyping is a technique used for the preparation of with well defined architecture scaffolds. Stereolithography, 3D printing and laser sintering are considered as rapid prototyping applications. All of them will yield a highly porous, specially designed structure by the help of computer programming.

There are several other scaffold fabrication techniques like gas foaming and peptide self assembly. The choice of fabrication technique can give control on the porosity, pore size and interconnectivity of

the pores, and with proper choice of material the prepared scaffold will serve to create an engineered tissue with all the functions of the target tissue [60, 61].

1.4.2.   Materials Used In Scaffold Fabrication

Materials with different properties have been used to construct the desired tissue by providing a support for the cells to attach and grow. For tissue engineering applications, many materials of natural or synthetic origin have been used.

Natural materials are preferred due to their similarity to targeted tissues; they are either found in the structure of the target tissue, or have a similar property. This similarity to the natural tissue allows cells to behave as they do in their natural environment and this is important because their function is affected by the surrounding ECM. Common examples of natural materials used in tissue engineering are organic polymers like different types of collagen, especially types I and II, silk, gelatin, glycosaminoglycans, alginate and chitosan, or inorganic natural materials like hydroxyapatite. Despite the excellent cell support and ECM mimicry, use of natural origin materials has some limitations. The mechanical properties of natural polymers are generally poor. Furthermore, the availability of these materials depends on the natural sources they are obtained from and generally these sources are limited. Also, the isolation processes of natural polymers do not yield uniform chain lengths due to the process, or source (species differences, age, sex, etc.) of the polymer [28, 34, 62]. In order to bring a solution to the problem of limited sources and heterogeneity of the natural polymers, recombinant polymers like recombinant human collagens are used [63].

To avoid the problems encountered with natural polymers, biocompatible synthetic polymers are utilized for tissue engineering purposes. The most frequently used examples of synthetic polymers are poly(glycolic acid) (PGA), poly(lactic acid) (PLA), poly(lactic-co-glycolic acid) (PLGA), poly(ε-caprolactone) (PCL), poly(3-hydroxybutyrate) (PHB) and poly(3-hydroxybutyrate-co-3-hydroxyvalerate) (PHBV). Synthetic polymers can be produced in large amounts reproducibly and their composition and properties can be modified as needed. However, these polymers generally do not encourage cell attachment and growth as natural polymers do. Moreover, the acidic degradation products of synthetic polyesters were reported to cause inflammatory responses in the surrounding tissue due to decreased local pH [60, 64].

1.4.2.1. Collagen

1.4.2.1.1.   Structure, Function and Sources of Collagen

Since the most abundant protein in the structure of cornea is collagen, most of the corneal tissue engineering constructs are made up of, or contain collagen. Poor mechanical strength of the scaffold is not a big challenge when cornea is considered. It is a soft tissue which does not require the superior load bearing characteristics like bone or tendon would.

Proteins belonging to collagen family constitute the largest fraction of the ECM composition [65, 66]. Collagens consist of more than 20 different types. Collagen is a fibrous protein, made of a right-handed triple helix of 3 left-handed helices. The three helices of collagen are stabilized by interchain crosslinks, covalent and hydrogen bonds. It is a large protein, made up of about 1000 amino acids. The common sequence of collagen is -Ala-Gly-Pro-Arg-Gly-Glu-4Hyp-Gly-Pro- [66, 67]. The amino acid 4-hydroxyproline (4Hyp) is a derivative of proline (Pro) and it is a characteristic marker of collagen because no other protein contains such high fractions of glycine in their structure [68]. Also, abundance of high glycine content (about 30%) is another distinctive property of collagens.

Among the many different types of collagen, type I, II, III and V are the most abundant ones as they are the main components of bone, muscle, skin, tendon and cartilage [68]. These fibrillar proteins are mostly involved in the protection of the tissue integrity and increase of strentgth. Since they form a considerable portion of the extracellular matrix of tissues, they present a large surface for cell attachment and growth. They also serve as basement membranes too, in various tissues like cornea.

Moreover, along with glycosaminoglycans (GAG) they are in contact with, collagen contributes to compressive and tensile characteristics of the tissues [66-68]. In addition to mechanical functions, collagen is important in tissue repair and organ development as the interaction of cells with collagen trigger the molecular pathways to activate specific growth factors [65].

Collagen used in tissue engineering is mostly derived from animal sources like bovine skin and tendon, porcine skin and rat tail [66]. Recombinant human collagen is also produced and used as well as xenogenic sources [46]. The purity of collagen has become an important issue especially after mad cow disease.
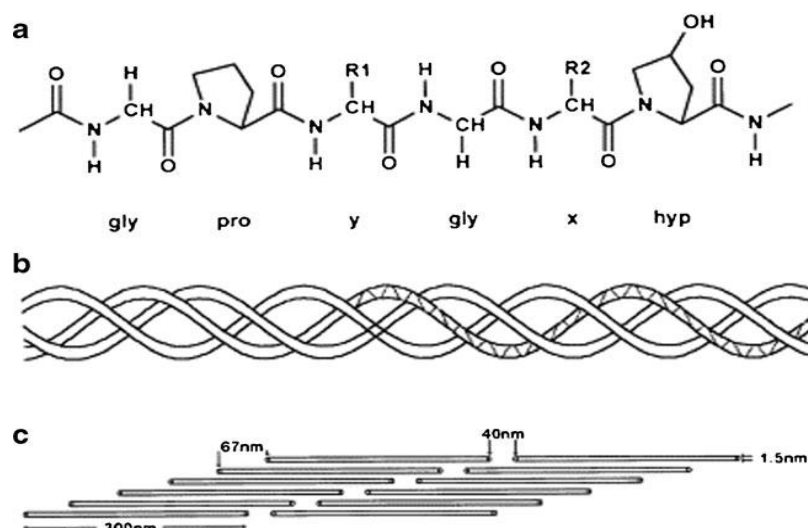
Figure 1. 5. Schematic diagram of Type I collagen structure (adapted from Fullana and Wnek, 2012)

1.4.2.1.2.   Collagen Use in Tissue Engineering

Collagens, especially collagen type I, are highly preferred for tissue engineering applications but there are also a few drawbacks; such as the low mechanical strenghth during the period when the neotissue is being produced [69]. In order to compensate for this crosslinking techniques are used to construct durable collagen based scaffolds. Crosslinking methods can be grouped as physical, chemical, and enzymatic. Most commonly used physical crosslinking methods are UV exposure and dehydrothermal (DHT) treatment [70]. DHT treatment is more widespread in tissue engineering and it leads to the formation of covalent bonds between collagen molecules by decreasing the water content with exposure to high heat for several hours [69, 70]. As indicated in the study of Pieper *et al*, DHT treated (80°C, 48h) collagen based porous scaffolds showed increased tensile strength as compared to untreated samples [71]. In another study Kınıkoğlu et al., used DHT treatment (145°C, 48 h) to stabilize the collagen based electrospun fibers prepared for tissue engineering applications. The results indicated that the treated samples preserved their fibrous structure when incubated in aqueous medium [72].

Other chemical crosslinking methods utilize carbodiimides or aldehydes. Aldehydes like glutaraldehyde or formaldehyde have been extensively used, however, there are concerns about the cytotoxicity unreacted compound remaining behind. This toxic effect can be minimized by exposing the scaffolds to lower concentrations of the compound, treating with certain compounds to passivate them or use other less toxic materials. Another common chemical used for crosslinking is N-ethyl-N-(3-dimethylaminopropyl)carbodiimide) (EDC), which is mostly used in combination with N-hydroxysuccinimide (NHS). The crosslink mechanism of EDC/NHS is shown in Figure 1.6. Briefly EDC reacts with the carboxylic acid group in collagen and forms an active, unstable intermediate, which can react with an amine group on the same or another collagen molecule, forming a stable

amide crosslink. However, the intermediate may go through hydrolysis, especially in aqueous solutions like growth mediums used in tissue engineering processes or in the body environment. This instability is prevented by the addition of NHS, which converts the intermediate into NHS-ester; thus EDC-mediated crosslinking efficiency increases.

This method is favorable since the EDC itself does not remain behind as a part of the crosslinked molecule and the resulting end product is a derivative of urea, which can be metabolized safely. As a result EDC/NHS can be used to crosslink collagen without changing the carboxylic end of the molecule, and the residues can be easily washed off [73].
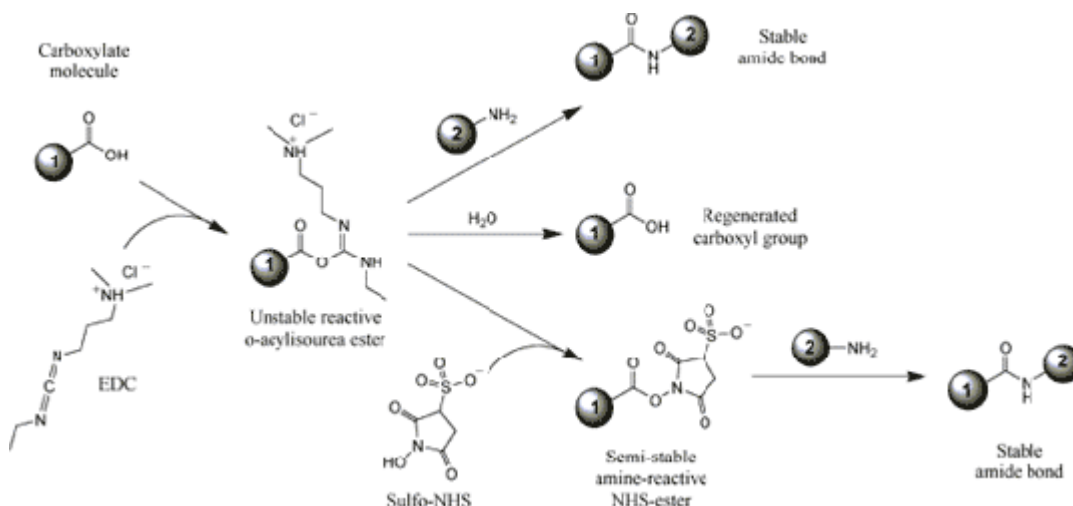
Figure 1. 6. EDC/NHS crosslinking mechanism [73]

Finally enzymatic crosslinking can be used without any cytotoxicity. An example of such enzymes is transglutaminase, which improves tensile strength, when applied to the scaffold [69].

Collagen whether blended with another polymer or alone, has been used in various scaffold forms. Most common forms prepared are foams, films, hydrogels and fibers. The tissue engineering applications of collagen include skin, cartilage, bone, tendon, heart valve, neural tissues, cornea etc.

80% of the dry weight of skin is constituted by collagen type I, for this reason some substitutes of collagen type I are extensively constructed. Most important ones among these are wound dressings. The most popular artificial skin based on collagen type I is Apligraf® [74], which is a collagen layer seeded with fibroblast, and an overlying epidermis substitute seeded with keratinocytes. Another commercialized example is Integra®, a collagen-GAG scaffold without cells.

Collagen type II is the main constituent of cartilage; this is in contrast to many other tissues which have collagen type I as the major ECM component. Collagen type II is therefore the main compound used in cartilage tissue engineering [68]. Mizuno and Glowacki [70], showed the effect of collagen and demineralized bone powder on the induction of fibroblast differentiation into chondrocytes. Among the many biocompatible materials they have tested, many, except collagen, inhibited the desired effect.

Bone is a highly mineralized tissue and the majority of its dry weight is constituted by collagen type I and hydroxyapatite (HA). 3D scaffolds of collagen type I and hydroxyapatite, therefore, have been frequently tested in bone engineering studies. Incorporation of HA increased the mechanical strength and cell attachment [68]. In a fibrous scaffold made up of blend of PCL, collagen type I and HA, collagen/HA had the greatest Young's modulus indicating higher mechanical properties, especially stiffness [75].

Tendon is another collagen rich tissue in the structure of which fibers are arranged longitudinally. This arrangement of collagen fibers enable the tissue to endure great tensile stresses [68]. Butler *et al.*, (2006) have used porous collagen type I sponges to accommodate bone marrow stem cells, and the resulting culture had 75% of the strength of the native tendon in 12 weeks [76].

Heart valves, are also mainly composed of collagen type I and they are mimicked by construction of collagen based scaffolds. Pandit and colleagues designed a collagen based 3D gel and incorporated a co-culture of porcine heart valve interstitial cells and endothelial cells [53]. The tissue specific extracellular matrix deposition was observed when the cells are grown in/on the prepared gel, thus collagen based scaffolds are suitable as heart valve tissue engineering constructs.

Collagen based nerve conduits are also shown to be effective in nerve regeneration. A collagen based nerve tube constructed by Madison and coworkers [77] was tested *in vivo* in rodents and primate. Results suggest that collagen based scaffolds hold promise as the regeneration was as successful as clinical autografts in terms of recovery of sensory nerve and target muscle responses.

Cornea is another collagen rich tissue and therefore collagen is a material of choice in tissue engineering of corneal constructs. Details of collagen use in corneal tissue engineering are presented in Section 1.4.

1.4.2.2. Chondroitin Sulfate

1.4.2.2.1.   Structure and Function of Chondroitin Sulfate

Chondroitin sulfate (CS) is an anionic polysaccharide found in proteoglycans and in the ECM of many tissues like cartilage, bone, skin and heart valves as well as in cornea. It is a linear polysaccharide with a number of different repeating disaccharides, to yield chondroitin sulfate, dermatan sulfate, chondroitin 4-sulfate, chondroitin 6-sulfate, chondroitin-4,6-sulfate and chondroitin-2,6-sulfate [79]. It is linked to protein backbone of the proteoglycans. The chemical structure of chondroitin 4-sulfate is shown in Figure 1.7.
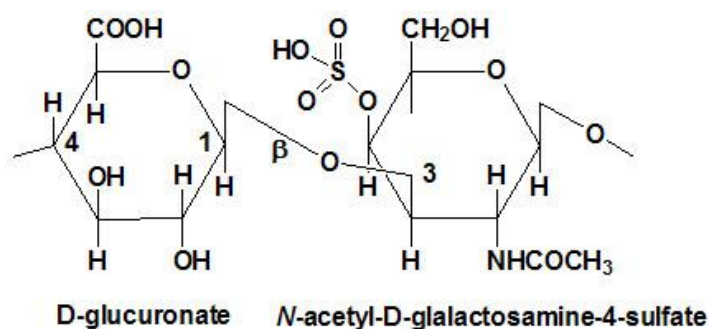
Figure 1. 7. Structure of chondroitin 4-sulfate constituted of repeating units of β-D-glucuronate and N-acetylgalactosamine-4-sulfate. (Adapted from: http://themedicalbiochemistrypage.org/glycans.php) [78]

Chondroitin sulfate, like other glycosaminoglycans, functions as a lubricant due to its ionic nature, holds significant amount of water and is important for the ECM organization [79, 80]. They are found in cartilage, bones, and the cornea; cartilage, umbilical cord, and tendon; skin and the lungs respectively. Moreover, being bound to a protein backbone and being able to bind water and cations, due to their anionic nature, glycosaminoglycans like chondroitin sulfate provide viscoelasticity to tissues [80]. The function of CS rich tissues are affected by the presence, type and concentration of chondroitin sulfate in the surrounding matrix.

1.5.   Corneal Tissue Engineering Approaches

Among the various types of tissue engineering scaffolds used the most common ones are hydrogels, decellularized structures, films with or without patterns and foams [81-96]. Hydrogels of polymers like PHEMA, collagen, collagen-PVA composites or biofunctionalized collagen have been tested [84-88]. Decellularization of tissues resulted in porous native ECM structures and these structures were also tested as corneal tissue engineering scaffolds. Examples include the use of decellularized bovine and porcine cornea and human amniotic membrane [89-91]. Another common scaffold form used in corneal tissue engineering is film. Films of collagen, poly(L-lactide-co-D,L-lactide) (PLLA)/PHBV mixture, silk and collagen–gelatin–hyaluronic acid composites were tested for use in corneal reconstruction [92-95].

Since the most commonly used material and scaffold type for corneal reconstruction are collagen type I and porous foams, respectively, the main focus of this section will be on the collagen based foams previously designed for corneal engineering applications. Although foams composed of different materials have been constructed [84, 96], collagen based foams were used.

As an important glycosaminoglycan component of cornea, chondroitin sulfate is frequently incorporated into corneal tissue engineering scaffolds to enhance cell attachment and to organize the collagen fiber orientation [83].

In a study by Griffith *et al.* [44], three types of cells were seeded onto a collagen-chondroitin sulfate scaffold, to prepare a full thickness corneal equivalent. The results showed that the construct accommodated all the cell types of the three layers of the cornea successfully. Further examination of characteristic features of cornea like transparency and cellular gene expression in the case of injury, proved that this scaffold containing chondroitin sulfate is suitable for use as a corneal tissue equivalent.

A collagen based scaffold was designed for construction of a full thickness corneal equivalent by Vrana and coworkers [39]. The collagen/chondroitin sulfate foam was prepared by lyophilization of the collagen solution followed by impregnation into chondroitin sulfate solution. The foam was crosslinked chemically by adding EDC/NHS into the collagen solution, and a second crosslinking was applied to the foam for the stabilization of chondroitin sulfate. Extensive scaffold characterization was made indicating the porosity, average pore size and thickness of the foams. In order to better mimic the natural cornea, the scaffolds were designed to have a similar thickness, an average of 530 μm. After chondroitin sulfate incorporation bulk porosity of the foams were approximately 85% with pores of 62 μm diameter in average. The capacity of the foams to accommodate all three cell types of cornea was tested *in vitro*. Isolated human corneal cell were used for construction of epithelial and stromal layers of the cornea and transfected human endothelial cells for endothelial reconstruction. All three layers were constructed successfully at the end of long incubation period (84 d), as histology results indicate. With the stratification of epithelial layer, as a result of air-liquid interphase, swelling of stroma and endothelial growth caused an increase in thickness of the construct. The Bowman's membrane and Descemet's membrane were not formed, however, the synthesis of marker corneal ECM proteins such as collagens type I, V and VI, and CD34, was observed. As a result a full thickness reconstructed cornea was successfully prepared [39].

In another study, a scaffold of hydroxypropyl chitosan, gelatin and chondroitin sulfate was tested for corneal tissue engineering [82]. Tested characteristics include ion permeability, transparency, light transmittance and biocompatibility of the scaffold. Results showed that the scaffolds with and without chondroitin sulfate were permeable to NaCl and glucose and had better transparency than the native cornea. The incorporation of chondroitin sulfate significantly enhanced cell growth, and thus the suitability of the scaffold for use as a corneal substitute.

Zhong *et al*. [83] also prepared a nanofibrous scaffold of collagen-chondroitin sulfate mixture. The fibers were produced by electrospinning and the resulting fibers had an average diameter (260 nm) close to that of native ECM fibers. The rabbit conjunctiva cells could be grown on the scaffold and

showed that the scaffold was not cytotoxic. Scaffolds containing chondroitin sulfate had a significantly better growth profile than those without chondroitin sulfate.

Orwin and Hubel [97] prepared collagen type I sponges by lyophilization and were then crosslinked by DHT. The scaffolds were much thicker (2-3 mm) than the native cornea. They were tested *in vitro* by seeding of endothelial cells, epithelial cells and stromal keratocytes separately or as co-cultures. The co-cultures involved the combination of two cell types, either epithelial cells/keratocytes or epithelial/endothelial cells. The single cell studies suggested that the collagen sponge was suitable for the growth of all three cell types as each behaved normally (layer formation by epithelial cells, ECM secretion by keratocytes, and monolayer formation of endothelial cells). The co-culture studies on the other hand, gave insight on the compatibility of the different cell types on each other. In both co-culture designs the presence of a second cell type promoted the stratification of the epithelial layer. The results showed that the epithelial cells formed only 2 layers when seeded without co-culturing with endothelial cells or keratocytes but 4 layers in the co-culture.

Haskell *et al.,* [98] used collagen sponges with different collagen densities biofunctionalized with chondroitin sulfate. Human corneal fibroblast seeded scaffolds were cultured in a bioreactor. The histology tests showed that the cells penetrated into and attached to the scaffold, and optical test results showed that as the density of the constructs decreased so did their light scattering, just like in the native cornea.

Vrana et al., [99] presented crosslinked collagen foams prepared by lyophilization and crosslinked chemically by EDC/NHS. Crosslinked samples were roughly 800μ thick and had a porosity of 94% in average. The foams showed 80% weight loss by the end of the 4th week of incubation in PBS at 37ºC. Primary human corneal keratocytes increased in time and cells penetrated deeper into the sponges as was shown by the positive staining of the cell nuclei. Immunostaining indicated that all of the marker proteins for the characteristic components of ECM, collagen type I, V and VI were synthesized by the corneal keratocytes and secreted as the new extracellular matrix.

1.6.   The Approach and Novelty of This Study

In the many tissue engineering studies towards the construction of a corneal equivalent, either full or split thickness, mimicking the formation of the Bowman's membrane was not attempted. In this study the aim was to produce a split thickness corneal construct consisting of the epithelial and stromal layers. The construct was composed of a stromal layer of crosslinked collagen/chondroitin sulfate foam and isolated human keratocytes cells foam and an epithelial layer of retinal pigment epithelial cells (D407) seeded on a fibrous mat of collagen type I attached onto the foam. By seeding the epithelial cells onto the electrospun fiber layer, the fibers were expected to serve as the Bowman's membrane. The presence of this fibrous layer was expected to enhance epithelial cell-keratocyte contact by supporting and physically separating the two cell types. This is known to be important for the maturation of the construct for clinical applications as the interaction of the two cell types when seeded onto a scaffold without a separating layer between them delays the formation of a new Bowman's membrane by the epithelial cells [100].

2. MATERIALS AND METHODS

2.1. Materials

N-ethyl-N-[3-dimethylaminopropyl]carbodiimide (EDC), *N*-hydroxysuccinimide (NHS), chondroitin sulfate A (CS) (from bovine trachea), Coomassie brilliant blue, amphotericin B, 1,1,1,3,3,3-hexafluoroisopropanol (HFIP), collagen Type I, paraformaldehyde (37%), FITC-labeled phalloidin, 4,6-diamidino-2-phenylindole dihydrochloride (DAPI), mouse anti-human collagen Type I, and Alexifluor532 conjugated anti-mouse Ig antibody were purchased from Sigma (USA and Germany).

Sodium phosphate monobasic and dibasic, sodium chloride (NaCl), dimethylformamide (DMF), ethanol, acetic acid (HAc), acetone, and Tween-20 were purchased from Merck Millipore (Germany).

Fetal calf serum and DMEM/F12 (1:1) (Dulbecco's Modified Eagle Medium (DMEM; high glucose) and Ham's F12 medium) were supplied by Hyclone, Thermo Scientific (USA).

New born calf serum was supplied by Lonza (Sweden). Collagenase Type II was obtained from GIBCO (USA).

Penicillin/streptomycin (Pen/Strep) (100 units/mL - 100 μg/mL), and bovine serum albumin (BSA) were purchased from Fluka (Switzerland).

Dimethyl sulfoxide (DMSO) and Triton-X 100 were obtained from AppliChem (Germany).

Basic fibroblast growth factor (b-FGF), Trypan blue (0.4%) and Alamar blue® were purchased from Invitrogen Inc. (USA).

Sprague-Dawley rat tails to extract collagen type I were a kind gift of Tayfun Ide from GATA Animal Experiments Laboratory (Ankara, Turkey).

2.2. Methods

2.2.1. Collagen Type I Isolation from Rat Tails

Isolation of type I collagen from rat tail was performed according to the procedure previously described by Vrana *et al.,* 2008. Briefly, the tendons in the tail were removed after the skin was stripped away. The collagen in the tendons was dissolved by acetic acid treatment (0.5 M). Insoluble fatty tissue was removed via glass wool filtration. Further purification of the collagen was achieved by dialysis against the buffer (12.5 mM sodium phosphate dibasic, 11.5 mM sodium phosphate monobasic, pH 7.2) which was renewed daily for a total of 7 days. The collagen solution was centrifuged (Sigma 3K30, Germany) (16,000 g, 10 min, 4 ºC) and the pellet was collected. When the pellet was completely dissolved with acetic acid treatment (0.15 M), it was precipitated with NaCl addition (5% w/v). Following a second centrifugation step, the pellet was dissolved in acetic acid solution and dialyzed under the same conditions with the first dialysis for another 7 days. Second dialysis was followed by a centrifugation step and the resulting pellet was stored in 70% ethanol for 2 days. The precipitated collagen was centrifuged and the pellet was frozen (-80 ºC, Sanyo MDF-U53865, Japan) and then lyophilized (FreeZone 6, Labconco Co., USA) and stored in this state at 4 ºC.

2.2.2. Preparation of Scaffolds

#### 2.2.2.1. Preparation of Crosslinked Collagen Foams (XLF)

Isolated type I rat tail collagen (0.3%) was dissolved in 0.2% acetic acid overnight. Crosslinker solution with a w/w ratio of 1:1:1.3 (collagen:NHS:EDC) was prepared. The two solutions were mixed and poured into the wells and stored for 2 h at room temperature (RT, 25 ºC) for crosslinking. Samples were frozen overnight and then lyophilized for 8 h.

2.2.2.2. Preparation of Chondroitin Sulfate Impregnated Collagen Foams (CSXLF)

Chondroitin sulfate (CS) solution was prepared (3 mg/ml chondroitin sulfate in distilled water (dH$_2$O)). The CS solution was added onto the foams and maintained in this form for 30 - 45 min at room temperature (RT). The CS solution was removed and the foams were frozen and lyophilized for 8 h. Crosslinker solution (33 mM EDC, 6 mM NHS in NaH$_2$PO$_4$ pH 5.5) was prepared and poured onto the foams. Crosslinking was completed in 2 h at RT. Foams were washed with Na$_2$HPO$_4$ (0,1 M, pH: 9,1), NaCl (2M), NaCl (1M) and dH$_2$O at RT. The chondroitin sulfate impregnated foams (CSXLF) were frozen and lyophilized for 8 h. An additional crosslinking step was carried out to be able to test the effect of presence of fiber layer on cell growth and morphology by comparing same scaffolds with and without fiber layer. CSXLFs were dehydrothermally crosslinked at 150 ºC for 24 h.

2.2.2.3. Preparation of Foam-Fiber Scaffolds

Collagen solution (9% collagen and 1% DMF in HFIP) was prepared and electrospun onto the foams which were pinned onto the aluminum collector. With the stabilization of fibers by DHT treatment (150 ºC, 24 h) the foam-fiber construct (Fo-Fi) was completed.
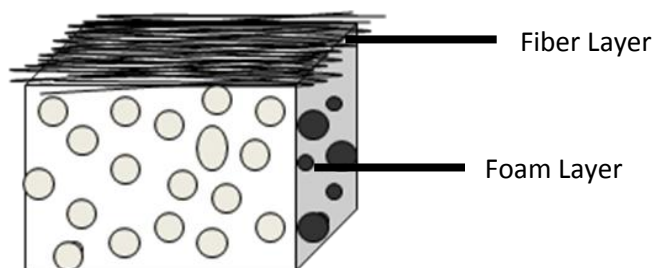
Figure 2. 1. Schematic representation of cross section of bilayer construct

2.2.3. Scaffold Characterization

2.2.3.1. Measurement of Thickness

Foam thicknesses, in dry and wet states, were measured using a standard micrometer (Erste Qualitat, Germany) to a sensitivity of 0.1 μm. Five replicate samples were used for each state and at least 3 measurements were done on each sample.

2.2.3.2. Measurement of Porosity

Surface porosity of XLFs and CSXLFs were determined by the NIH image J (USA) analysis program on stereomicroscope (Nikon SMZ 1900) micrographs. Four samples were used for each foam type.

2.2.3.3. Pore Size Distribution of Foams

Mercury porosimetry (Quantachrome Corporation, Poremaster 60, USA) analysis under low pressure conditions was used in order to measure the pore size distribution of XLFs to examine the effect of freezing temperature on pore size. The same analysis was carried out to examine the effect of DHT crosslinking on pore sizes of CSXLFs.

2.2.3.4. Stability of Foams

2.2.3.4.1. Collagenase Degradation Test

The stability of foams against collagenase activity was determined by gravimetric measurements. Four samples of XLFs, CSXLFs, Fo-Fi constructs and uncrosslinked foams (as negative control) were incubated in collagenase type II solution (0.1 mg/mL in PBS pH 7.4) for 2 h. The samples were washed, lyophilized and weighed to compare the weight loss of the samples.

2.2.3.4.2. Scaffold Degradation *In Situ*

Scaffolds were incubated in 10 mM PBS (pH 7.4) at 37 °C for 4 weeks. Gravimetric measurements were made at time points 0, 1, 2 and 4 weeks in order to obtain the degradation profile.

2.2.3.5. Light Transmittance and Transparency

Light transmittance of CSXLFs and Fo-Fi samples were determined by measuring the absorbance of the samples between 250 nm to 700 nm using a Shimadzu 2100-S UV-visible spectrophotometer. The transmittance values were then calculated by the equation:

Absorbance = 1/Transmittance

The transparency of CSXLF and Fo-Fi construct samples were tested by visual observation. The samples in wet state were placed onto a printed text of 12 font and the ease of the reading through the scaffolds was studied via their respective stereomicrographs.

2.2.3.6. SEM examination

All scaffold types were platinum-gold coated under vacuum with a sputter coating device (SEC, Mini-SEM Coating Device, South Korea) and observed with a scanning electron microscope (SEC, Mini-SEM, South Korea).

2.2.4. In Vitro Studies

2.2.4.1. Cell Culture

Both keratocytes and retinal pigment epithelium cells (RPE) were stored frozen at -80 °C in a mixture of their medium and DMSO (15%). The cells were thawed and incubated under standard conditions (37 °C, 5% CO_2) until they reached confluency. Cells were passaged once before they were seeded onto the scaffolds.

2.2.4.1.1. Keratocyte Culture

Isolated human keratocytes (P8-13) were used in all experiments. The composition of a 500 mL medium used for keratocytes was 450 mL of DMEM/F-12 (1:1 mixture of DMEM and Ham's F-12), new born calf serum (10%), 10 ng/mL human recombinant b-FGF, amphotericin B (1 µg/mL), streptomycin (100 µg/mL) and penicillin (100 UI/mL).

2.2.4.1.2. Retinal Pigment Epithelium Culture

D407 cell line of retinal pigment epithelium (RPE) (P11-18) was used in the experiments. The composition of 500 mL medium was as contained 475 mL of DMEM high glucose, fetal calf serum (5%), amphotericin B (1 µg/mL), streptomycin (100 µg/mL) and penicillin (100 UI/mL).

2.2.4.1.3. Co-culture

Co-culture of the two above mentioned cells was performed. The growth medium for co-culture was prepared by mixing their respective media at a 1:1 ratio.

2.2.4.2. Cell Seeding onto Scaffolds

Cells were treated with 0.05% trypsin (5 min at 37 °C) to be detached from the tissue culture plate. Following the inactivation of trypsin with medium addition, cells were collected by centrifugation. Cells were then counted with a hemocytometer and diluted to contain $2x10^5$ cells in 50 μL of suspension. CSXLFs and the foam side of Fo-Fi constructs were seeded with keratocytes. Cell seeded scaffolds were incubated for 1 h for cell attachment, and then medium was added to cover the scaffolds. The Fo-Fi samples seeded only with human keratocytes (Fo-Fi HK) and only with RPE cells (Fo-Fi RPE) were incubated in their respective mediums without further treatments. After 7 days of culture, the co-culture samples were seeded with RPE cells ($2x10^5$ cells/scaffold) on the opposite side of CSXLFs and on the fiber side of Fo-Fi co-culture constructs. The epithelial layer stratification was induced by placing the constructs at the liquid-air interface until the 14th day of culture. The immunostaining of the co-culture seeded constructs was carried out at the end of 14 days of culture. The transparency and light transmittance test was carried out at the end of 31 days of culture. The other scaffolds were used on their 14th day of incubation for testing, if not indicated otherwise.

2.2.4.3. Cell Proliferation on Scaffolds

Alamar Blue assay was used to determine the proliferation profile of both cells at 1, 7 and 14 days of culture. In order to observe the proliferation of both cells, samples seeded only with keratocytes, samples seeded only with RPE cells and samples seeded with both cell types were used. After the cell seeded scaffolds were washed off the medium, they were incubated with Alamar Blue solution (10%) at 37 °C and 5% CO_2 for 1 h. Then 200 μL of Alamar Blue solution was transferred into a 96 well-plate, and the absorbance of all solutions was recorded at both 570 nm (λ_1) and 595 nm ($\lambda 2$) with an Elisa plate reader (Molecular Devices, USA). The percent reduction of the dye was calculated by the following equation:

$\lambda_1 = 570$ nm $\qquad\qquad\qquad$ $\lambda_2 = 595$ nm

$(\varepsilon_{ox})_{\lambda 2} = 117.216$ $\qquad\qquad$ $(\varepsilon_{red})_{\lambda 1} = 155.677$

$(\varepsilon_{ox})_{\lambda 1} = 80.586$ $\qquad\qquad$ $(\varepsilon_{red})_{\lambda 2} = 14.652$

$$\text{Percent Reduction} = \frac{((\varepsilon_{ox})_{\lambda_2} \times A_{\lambda_1}) - ((\varepsilon_{ox})_{\lambda 1} \times A_{\lambda 2})}{((\varepsilon_{red})_{\lambda 1} \times A'_{\lambda 2}) - ((\varepsilon_{red})_{\lambda 2} \times A'_{\lambda 1})} x100$$

($A_{\lambda 1}$= Absorbance of test well, $A_{\lambda 2}$= Absorbance of test well, $A'_{\lambda 1}$= Absorbance of negative control well (blank), $A'_{\lambda 2}$= Absorbance of negative control well).

The cell number on scaffolds was determined from a calibration curve constructed using the same procedure with known number of cells.

2.2.4.4. Microscopy of the Tissue Engineered Construct

2.2.4.4.1. Staining the Cells with FITC-Labeled Phalloidin and DAPI

In order to study the cytoskeleton orientation and distribution of the cells, keratocyte and RPE cell seeded CSXLFs and Fo-Fi constructs and only keratocyte or RPE cell seeded Fo-Fi constructs were fixed Days 1, 7 and 14 of incubation with paraformaldehyde for 15 min. After washing with PBS, cell membranes were permeabilized with 1% Triton-X100 solution for 5 min. Next the samples were washed with PBS and then the samples were incubated in 1% BSA solution (in PBS, at 37 °C, 30 min). After washing with 0.1% BSA, FITC labeled phalloidin (1:100 dilution in 0.1% PBS-BSA) was added and samples were incubated at 37 °C for 1 h in dark.

The samples were washed with 0.1% BSA again and counterstained with DAPI (diluted 1:1000 in PBS) for 10 min at room temperature in dark. Finally, specimens were rinsed with PBS and examined

using an Zeiss fluorescence microscope (with Colibri LED light source system, Germany) with 365 nm LED module for DAPI and 488 nm LED module for FITC labeled phalloidin and confocal laser scanning microscope (Zeiss LSM 9100, Germany) with WB filter (450-480 nm).

2.2.4.4.2. SEM

Cell seeded CSXLFs and Fo-Fi samples were usedon Day 14 of incubation for SEM imaging. The samples were washed with PBS and then with cacodylate buffer (0.1 M sodium cacodylate, pH 7.4). They were fixed in paraformaldehyde (2.5% v/v in cacodylate buffer) at room temperature for 2 h. After washing with cacodylate buffer and distilled water, the scaffolds were freeze-dried, and treated as in section 2.2.3.6.

2.2.4.5. Immunostaining

2.2.4.5.1. Collagen Type I Staining

Anti-collagen type I antibody was used for the indirect immunostaining of cell seeded constructs. Collagen type I secretion by keratocytes and RPE cells was observed by this method on Day 1, 7 and 14 of incubation.

The samples were treated as in Section 2.2.4.4.1 up to DAPI staining step. Then the samples were incubated in the blocking solution (0.5% BSA, 0.1% FCS, 0.1% Tween 20 and 0.1% sodium azide in PBS). Anti-human collagen type I antibody produced in mice (1:100 dilution in 0.1% PBS/BSA solution) was then added onto the specimens and incubated for 1 h at 37 °C. After washing with 0.1% PBS-BSA solution they were incubated in Alexifluor 532-labelled Anti-mouse antibody produced in goat (1:100 dilution in 0.1% BSA-PBS) at 37 °C for another hour and then washed with 0.1% PBS-BSA solution. Samples were observed using confocal laser scanning microscope (Zeiss LSM 9100, Germany) between 500-550 nm with 488 nm Argon laser for cytoskeleton and between 555-650 nm with 532 nm Argon laser for deposited collagen.

2.2.4.6. Transparency and Light Transmittance of the Cell Seeded Construct

Transparency and light transmittance of the cell seeded constructs were examined using the method described in Section 2.2.3.5.

2.2.4.7. Suturability Testing

The suturability test was carried out by suturing a bilayer scaffold in its 31 days of co-culture with a prolene suture with cutting needle (6/0, blue). The durability of the construct was examined by stereomicrographs.

2.3. Statistical Analysis

Statistical analysis was carried out by the Student's t-test; $p \leq 0.05$ was considered significant.

CHAPTER 3

RESULTS AND DISCUSSION

3.1.   Characterization of the Collagen and the Scaffolds

The purity of the collagen type I isolated from rat tail was determined and characterization of the scaffolds, such as determination of thickness, pore structure and degradation profile was carried out.

3.1.1.   Characterization of Collagen Isolated from Rat Tail

The characterization of collagen type I isolated from Sprague-Dawley rat tails was carried out by SDS-PAGE method. The resulting bands of commercial collagen type I (Sigma, Germany) and the isolated collagen are shown in Figure 3.1. Approximate molecular weight determination was made by comparing, the isolated collagen (1st lane) with the protein ladder (Fermentas), presented in the 2nd lane and commercial collagen type I (3rd lane).
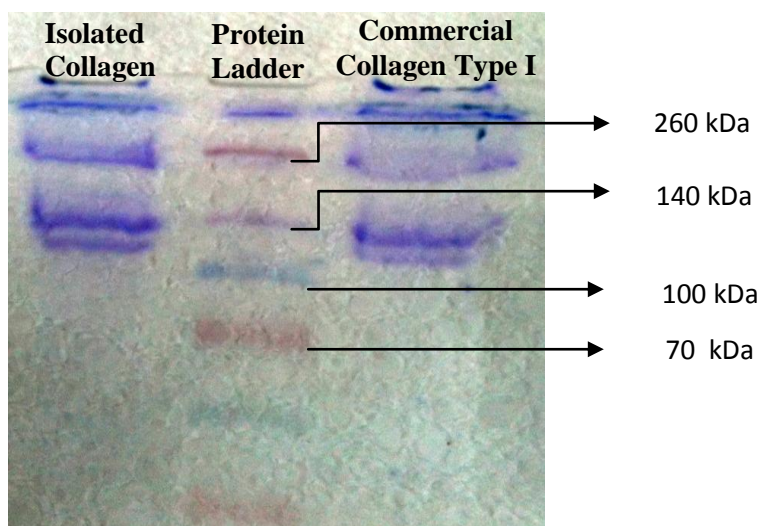
Figure 3. 1. SDS-PAGE results of collagens (I) isolated collagen (Source: Sprague-Dawley rat tails), (II) protein ladder (Fermentas), and (III) commercial collagen Type I (Sigma, Germany).

 The comparison of the two afore mentioned collagens shows that both the commercial and isolated collagens possessed 2 doublet bands around 140 kDa and 260 kDa. This result indicates that the isolated collagen is collagen type I. Since no other bands were obtained in the electrophoresis bands of neither collagen. This indicates that the collagen isolated from Sprague-Dawley rat tails was not only type I but was also pure.

3.1.2.   Characterization of Collagen Foams

The structure of the foams and bilayer scaffolds were examined under stereomicrograph and SEM and the results are represented in Figure 3.2 and Figure 3.8-3.11 respectively. Both examinations showed the porous nature of the foams and the fibrous structure collected on to the them clearly. The general structure of a non-chondroitin sulfate impregnated foam is shown in Figure 3.2 A and Figure 3.8. The

CS impregnated foams had a similar structure as shown in Figure 3.2 B and C, with higher porosity (see Section 3.1.3.). The fibers collected on to the foam were detectable by stereomicrographs at high magnifications when the bilayer and single layer constructs were compared (Figure 3.2 D and inset, respectively).
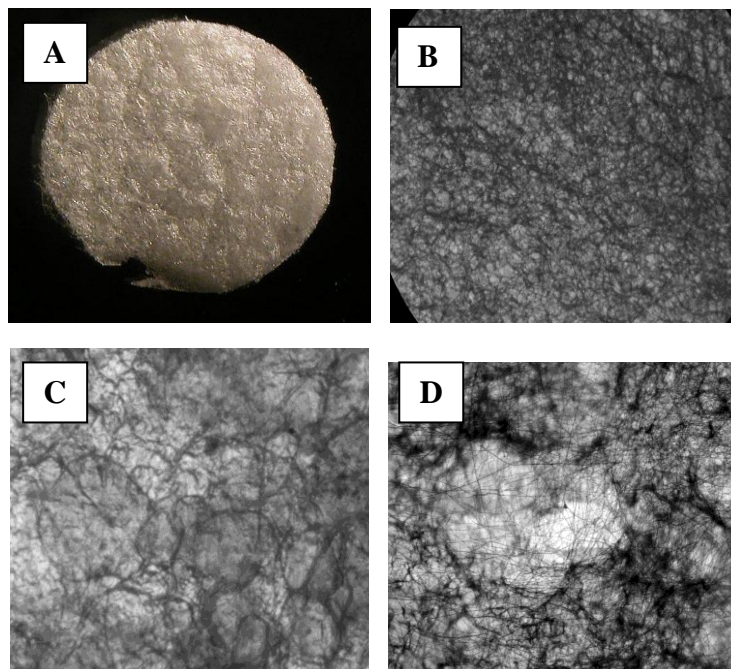
Figure 3. 2. General Structure of (A) XLF, (B) CSXLF before and (C) after DHT treatment, and (D) Fo-Fi construct.

3.1.2.1. Effect of Well Size on Foam Structure

Wells of two different diameters, 1.8 cm and 2.2 cm, were used in the preparation of the crosslinked foams (XLFs). The effect of the well size on the handling and structure of the collagen foams was determined. The thickness of the collagen solution was kept same by changing the volume. The foams prepared in the smaller wells using the same collagen concentration (0.3%) in acetic acid climbed on the walls of the wells due to surface tension and were also strongly attached to the bottom of the well, making removal and handling very hard. The climbing on the wall was significantly reduced when the wells had a larger diameter. Therefore, the foams prepared in wells with 2.2 cm diameter were used for further tests and treatments.

3.1.2.2. Effect of Freezing Temperature on Pore Size

In order to study the effect of the freezing temperature employed during lyophilization on pore size, foams were prepared by freezing at two different temperatures, -20°C and -80°C. The pore size distribution of the two respective foams was determined by mercury porosimetry. Moreover the stereomicrographs of the foams were compared to examine the surface pore characteristics of the foams. The results of mercury porosimeter analysis (Figure 3.4) suggest that both foams had a similar pore size range, from 10 μm to 200 μm. The majority of the pores had a diameter of approximately 200 μm. However, the fraction of the pores with diameters between 100 and 200 μm were higher in the foams prepared by freezing at -20°C. It is reported that there is an optimum pore size range for cells to attach and spread properly. A mean diameter of 180 μm was shown to be suitable for proper cell adherence, spreading and growth, as well as having the required mechanical properties [101, 102]. The pores with too large or too small diameters do not support effective cell attachment and growth [101]. A lower freezing temperature yielding larger pores is

24

consistent with literature [103]. At higher temperatures freezing is slower causing larger ice crystals, which will eventually lead to pore formation. Therefore the pores created by freezing the collagen solution at a higher freezing temperature such as -20°C leads to the production of larger pores [103, 104].

Interconnectivity of the pores is another one of the crucial needs for a tissue engineering construct mainly for proper material transfer through the construct [60]. Mid-sized pores provide the required interconnectivity and foams prepared by freezing at -20°C have a greater amount of mid-sized pores. Thus, one could expect these scaffolds to have better interconnectivity.

The stereomicrographs of the two foams are presented in Figure 3.3. They show that the foams prepared by freezing at -20°C have a more porous structure as also indicated in Figure 3.4. The pores of the -80°C frozen foam, however, do not have an open pore structure unlike the -20°C sample. The pores appear smaller and less in number suggesting that it has a poor interconnectivity, which is consistent with the mercury porosimeter analysis results.
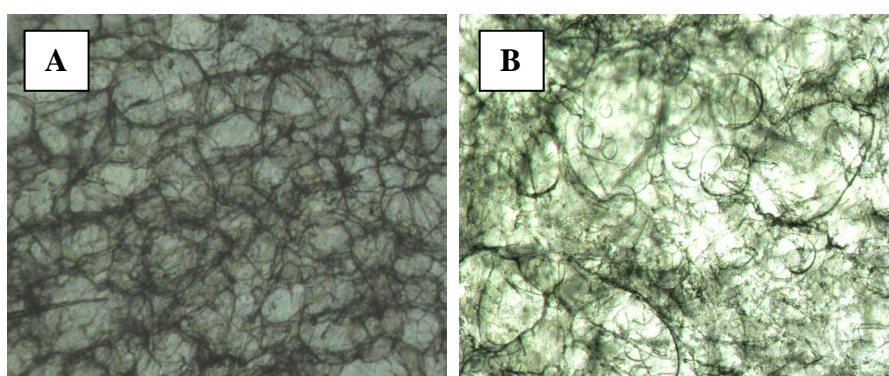
Figure 3. 3. Stereomicrographs of foams. Prepared by freezing at (A) -20°C, (B) -80°C. (Magnification was x60 for both)
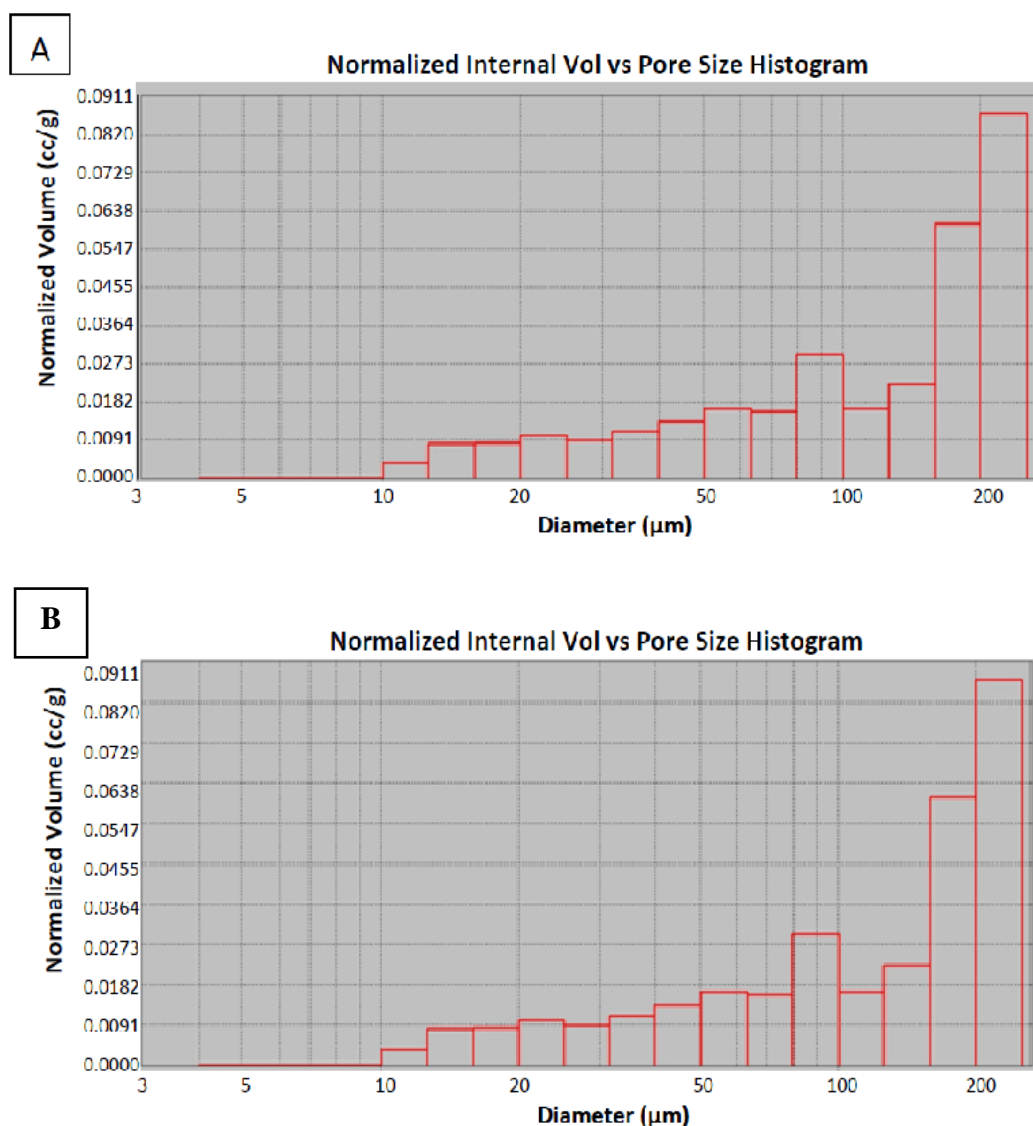
Figure 3. 4. Pore size distribution of XLFs prepared at (A) -20 °C, and (B) -80 °C.

As these results suggest, foams prepared by freezing at -20°C were chosen for further treatments and *in vitro* testing.

3.1.2.3. Porosity of Foams

The porosity of the foams was determined by analyzing stereomicrographs with ImageJ (NIH program). The porosity (%) of the dry foams is found to be around 70% which is quite suitable for cell penetration. (Table 3.1). The porosity of CSXLFs was significantly lower than that of the XLFs (p=0,033). However, following the DHT treatment it increases significantly (p=0.007).

Foam preparation whether with lyophilization or another method is known to cause layer formations at the bottom and the top surface of the scaffolds [106]. In a similar study, collagen-chondroitin sulfate foams prepared by lyophilization presented skin layer formation [39]. A similar skin layer formation was present in XLFs as presented in Figure 3.8. The reason behind CSXLFs having a lower porosity than XLFs is probably the impregnation with chondroitin sulfate. The increase in porosity following DHT treatment indicates thermal crosslinking shrinks the fibrils of

both collagen and CS leading to a more porous structure. Similar sponges of rat tail collagen type I have been prepared and their porosities were found to be close to the porosities of scaffolds prepared in this study. They have found that foams with approximately 63% surface porosity were suitable for cell attachment and growth [106], which is consistent with the cell proliferation results which will be presented later (section 3.2.1).

Table 3. 1. Porosity of Foams

Foam Type	Porosity (%)
XLF	66.7 ± 5.6
CSXLF without DHT treatment	56.6 ± 5.6
CSXLF with DHT treatment	69.6 ± 3.6

3.1.2.4. Pore Size Distribution of Foams

The pore size distribution of foams was determined with mercury porosimeter analysis and the results are shown in Figure 3.4 and Figure 3.5. To determine the pore size distribution and the effect of impregnation with chondroitin sulfate and crosslinking on pore size distribution, four samples of each foam type were examined. The XLFs were shown to have large pores with diameters around 200 μm. After the chondroitin sulfate impregnation process the fraction of small diameter pores (around 40 μm) was increased. The DHT treatment further decreased the pore sizes and homogeneity throughout the scaffold. In literature it was reported that unlike the results obtained in this study, chondroitin sulfate impregnation was shown to cause an increase in pore size [39]. However, the chondroitin sulfate impregnation was applied to a foam with much smaller pores than XLF samples used in this study. This was explained as the pore sizes of the foams were very small (35.6 μm) therefore, the second crosslinking step resulted in a selective crosslinking between smaller diameter pores, leaving out larger pores. As a result, the overall pore size increased following the impregnation process. In this study, however, the impregnation process was applied to a foam with much larger pores, probably resulting in a non-selective crosslinking. As a result the pores became smaller after chondroitin sulfate impregnation procedure. This result is consistent with literature as crosslinking is well known to cause a decrease in pore size [39, 106, 107]. It is also consistent with the porosity measurements (Table 3.1) and SEM micrographs of the scaffolds (Figure 3.8. and Figure 3.9). Another reason of decreased porosity can be the coating of the foam by chondroitin sulfate (Figure 3.9. A). After the DHT treatment the pore size further decreased showing consistency with literature as mentioned above.
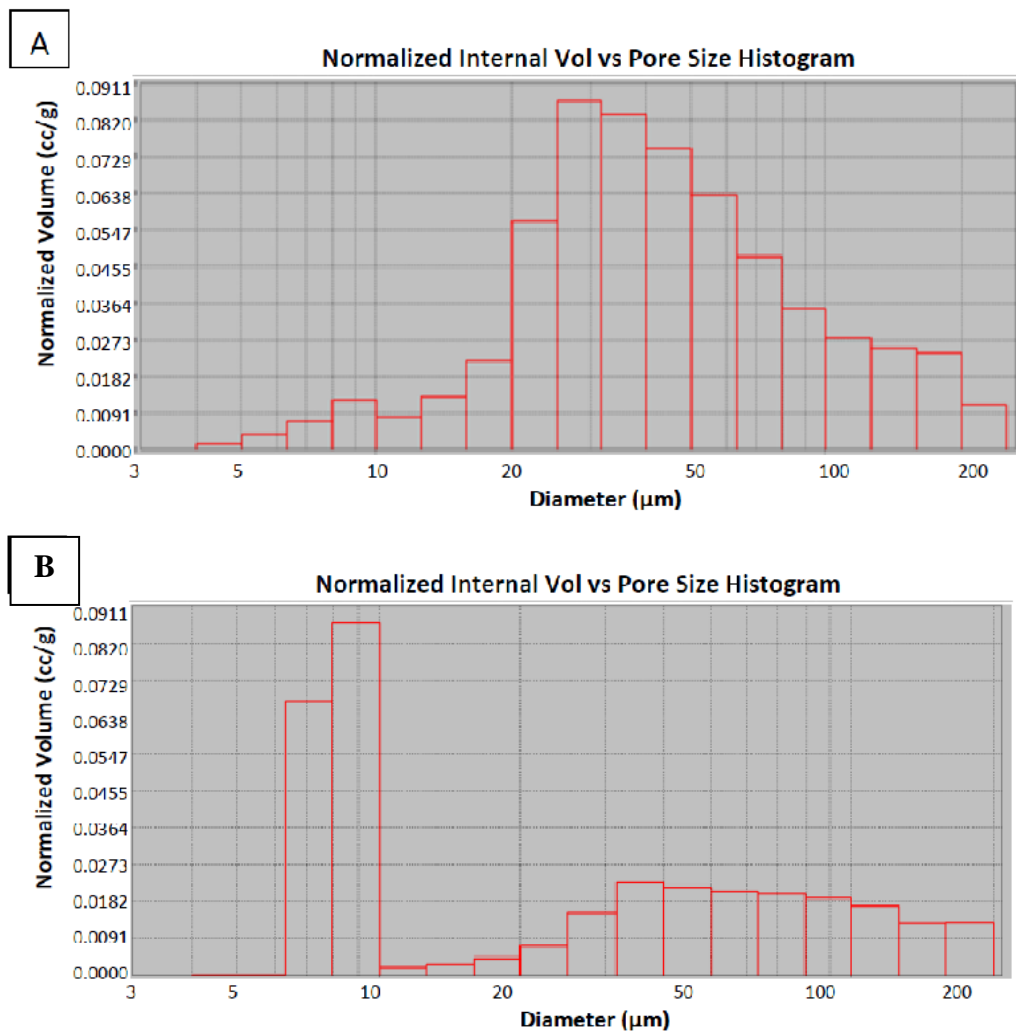
Figure 3. 5. Pore size distribution of CSXLFs. (A) without, and (B) with DHT treatment.

3.1.2.5. Thickness of Scaffolds

The CSXLFs and Fo-Fi constructs were prepared from XLFs by the procedure explained in sections 2.2.2.2 and 2.2.2.3 respectively. The thicknesses of these scaffolds were measured in dry and wet form. Moreover, the thickness of CSXLFs with and without DHT treatment was recorded to observe the effect of crosslinking on foam thickness. All thickness measurements were carried out by the method in section 2.2.3.1, and are presented in Table 3.2.

Since all the constructs are solely made up of collagen, they have a tendency to absorb water and swell [80, 108]. As expected the wet state thicknesses of the constructs were significantly higher than that of dry scaffolds due to swelling (p≤0.0001). All three types of scaffolds almost doubled their thicknesses when they are wet. DHT treatment did not lead to any significant change in the thickness of the foams in either dry or wet state. The thickness of Fo-Fi construct was expected to be close to DHT treated CSXLFs, since they are prepared by collecting collagen fibers on top of CSXLFs and finally DHT treated as a whole. The bilayer constructs were as thicker as the fiber layer's thickness. As the results show the thickness of the fiber layer is around 8 to 10 μm. The thickness of the fiber layer was aimed to be close to the thickness of natural Bowman's membrane (10 μm) [19] to better mimic the native cornea.

28

The final construct to have a thickness close to its native counterpart is desired [27]. Wet thickness of the scaffold is important to have a better estimate of the thickness of cell seeded constructs because the reconstructed cornea will be seeded with cells and incubated for several weeks in an aqueous medium for the tissue maturation. Therefore, the wet thicknesses of the constructs had to be close to native stromal thickness, 400 µm [2]. The results show that both the DHT treated CSXLFs and the Fo-Fi constructs have the targeted thicknesses and are therefore suitable as stroma substitutes.

Table 3. 2. Thickness of Scaffolds

State of Scaffold	Scaffold Type	Thickness (µm)
Wet State	CSXLF without DHT	394 ± 12
	CSXLF with DHT	391 ± 26
	Fo-Fi construct	401 ± 8
Dry State	CSXLF without DHT	220 ± 7
	CSXLF with DHT	217 ± 34
	Fo-Fi construct	225 ± 23

3.1.2.6. Stability of Foams

Tissue engineering primarily aims to replace or support a diseased or damaged tissue and help a new ECM deposition is made. The constructs are preferably degradable since new tissue is being formed to replace the artificial equivalent. Therefore, a tissue engineering construct should be stable in an aqueous medium for an 'appropriate' period of time, neither too long nor too short, appropriateness changing with the targeted tissue [29, 34]. Thus, the degradation profiles of the scaffolds prepared in this study were examined to test the suitability of the stability of the scaffolds for use in corneal tissue engineering.

3.1.2.6.1. Collagenase Degradation Test

The susceptibility of the collagen based scaffolds to collagenase was tested by treating the samples at 37°C with collagenase (0.1 mg/mL) activity and incubation in PBS (10 mM) was used as the control. (Table 3.3). The uncrosslinked foams and fibers were very fragile and disintegrated in the first 15 min of collagenase treatment. The only PBS treated foams lost around 75% of their weight at the end of a 2 h incubation. The PBS treated uncrosslinked fibers, however, were totally disintegrated at the end of two hours. On the other hand, the chondroitin sulfate impregnated samples showed a higher resistance to collagenase as CS are polysaccharides. The DHT treatment applied to CSXLFs did not lead to a significant improvement in the collagenase resistance of the scaffolds in the given duration (p≥0.05). Bilayer construct was not as strong as DHT treated CS carrying crosslinked foams (CSXLFs) and showed a greater weight loss (p≤0.05).

A tissue engineering construct should retain its mechanical and physical properties until ECM deposition by the cells start to take over the tissue equivalent [27]. Collagen based scaffolds, however, have a problem because corneal keratocytes are known to secrete proteolytic enzymes and these degrade collagen in time [109]. However, since ECM deposition should also be made by these cells, eventually a strong tissue has to form. Thus, the test when done in situ does not take into account the contribution of the cells to ECM. The in situ results are still important for the initial few weeks when ECM deposition is not significant yet.

The disintegration of uncrosslinked samples and resistance of their crosslinked equivalents are supported by literature [109, 110, 111]. In the study of Drexler *et al*., collagen type I isolated from bovine hide was used to prepare electrospun fibers. The fibers were then treated with different methods of crosslinking , DHT, EDC/NHS and both. They have shown that fibers lost their integrity upon incubation in the aqueous medium, for 3 h even in the absence of collagenase. Samples treated with DHT or EDC gained resistance against collagenase activity. When both treatments were applied the weight loss in 3 h was significantly decreased (45%) [112]. In the present study all the constructs showed a high resistance to collagenase treatment. This can be due to the application of EDC/NHS crosslinking procedure twice, followed by a DHT treatment. DHT treatment did not lead to a significant difference in collagenase susceptibility of the CSXLFs. This suggests that the scaffolds were sufficiently stabilized by the EDC/NHS treatments and there were not much functional groups left to further crosslink. The Fo-Fi constructs were more susceptible to collagenase treatment as the higher weight loss indicates. The foam layer of the construct is not as susceptible as the fiber layer to collagenase since it undergoes two extra crosslinking procedures. Therefore, when the CSXLFs and Fo-Fi constructs are compared, the weight loss of the latter is greater as the fiber layer is degraded more rapidly than the foam layer. Even though the bilayer constructs showed a lower resistance than CSXLF samples, the degradation rate was similar to or better than that of the other DHT treated foams [106, 110, 112].

Table 3. 3. Degradation of the fibers, foams and 3D construct by collagenase (at   37°C, 2h)

Scaffold Type	Weight Loss (%)	
	Collagenase (0.1 mg/mL) Treated	*Control
Uncrosslinked foam	100	70 ± 4
Uncrosslinked fiber	100	100
CSXLF without DHT treatment	13 ± 4	3 ± 2
CSXLF with DHT treatment	12 ± 3	4 ± 2
Fo-Fi Construct	30 ± 4	5 ± 2

*Control samples are treated with PBS (pH 7.4, 10 mM).

3.1.2.6.2.   Scaffold Degradation *In Situ*

The *in situ* degradation profiles of the constructs were examined by incubating them at 37 °C in PBS (pH 7.4, 10 mM) for 30 days and the results are presented in Table 3.4. The foams show a slightly higher (p≥ 0.05) stability throughout the 30 days than the bilayer construct. Approximately 40% of the CSXLFs have degraded in one month, whereas the bilayer constructs lost almost 70% of their total weight in the same time period. At the first time point the bilayer constructs degraded approximately 15% more than the foams, then the difference between their degradation profiles decreased to 6%. In the literature a similar degradation test was applied to crosslinked soluble and insoluble collagen type I foams [106, 109]. Both foams lost about 70% of their weight at the end of 4 weeks. The foams tested did not have any coating or a second layer on top. Therefore, the lower weight loss of the foam samples prepared in this study suggest that they can be used for longer incubations; this is good because extended culture of keratocytes is proven to enhance collagen type I deposition [39, 112]. The bilayer construct, on the other hand, shows a similar degradation profile with the above mentioned soluble and insoluble foams, but the main degradation is at the fiber layer.

Table 3. 4. Scaffold degradation *In Situ* (PBS, pH 7.4, 10mM)

Weight Loss (%)				
Sample Type	**Treatment Period (days)**			
	0	**7**	**14**	**30**
CSXLF with DHT treatment	0.0	11.2 ± 11	15.0 ± 7	36.6 ± 13
Fo-Fi	0.0	27.3 ± 10	38.2 ± 14	65.5 ± 10

### 3.1.2.7. Light Transmittance and Transparency

Cornea is a transparent tissue and its most important optical function is to transmit light to inner optical elements of the eye. Major need for an artificial cornea arises from the loss of transparency of the cornea. In all cases a tissue engineered construct should perform all vital functions of its natural equivalent to be used as a tissue replacement. Therefore, it is very important to study the light transmittance and transparency of both cell seeded and non-seeded constructs.

Light transmission of a normal human cornea between 450-600 nm wavelengths increases from 80% to 94%. Above 600 nm, light transmittance of the cornea reaches 98% [98]. The wavelengths lower than 300 nm, however, are absorbed by the cornea, especially the UV-B range (280-330 nm) (Figure 1, Appendix A) [9]. The light transmittance of cell-free CSXLFs and Fo-Fi constructs in wet state (wetted by immersing in distilled water) between 250 nm to 700 nm range was examined with a UV-Vis spectrophotometer (Figure 3.6). The transmittance from 250 nm up to 300 nm was (72-79%) lower, than the transmittance observed up to 700 nm (82%). This shows that all constructs absorb UV-B and UV-C and transmit a very high percentage of the light at higher wavelengths as does the native cornea.
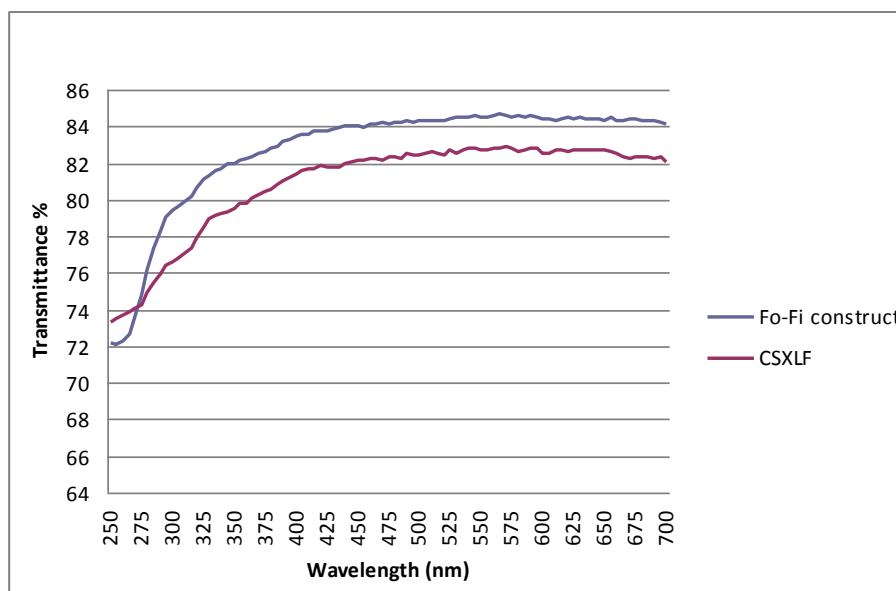
**Figure 3. 6.** Light transmittance of cell-free constructs.

In addition to light transmittance, the transparencies of the scaffolds were examined. Wet samples were placed on 12 font letters and the clarity of the writing was examined via stereomicrography. As Figure 3.7 shows both the CSXLF and Fo-Fi construct had good transparency as the words can be easily read through the wet foam and bilayer construct. Wet CSXLF, however, had a rougher surface when compared to bilayer construct.
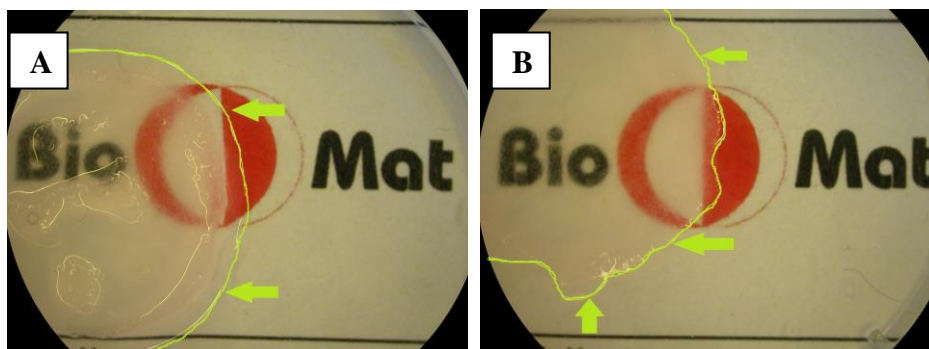

Figure 3. 7. Transparency of cell free (A) CSXLF, (B) Fo-Fi construct. (x7.5)

3.1.2.8. SEM Examination

The general appearance of all foams, fibers, and foam-fiber constructs were examined by SEM (Figure 3.8). The crosslinked uncoated foams had a skin layer, as the porosity measurements also suggested. Beneath the thin surface layer, a highly porous structure could be observed. After the DHT treatment, the CSXLFs showed a clear open pore structure (Figures 3.9 B and C), supporting the higher porosity of the constructs reported earlier (Table 3.1). The thermal treatment apparently caused the skin layer to disappear. To examine the bilayer scaffold, SEM micrographs of both sides of the construct were obtained. The foam layer of the constructs show the expected porous structure (Figures 3.10 A and B). Collecting the fibers on top of the foams did not have any effect on the foam structure. Single fibers were observed at the pores close to surface suggesting the fibers penetrated into the pores (Figure 3.10 A). However, it is clearly seen that fibers did not fill the pores, only few singe fibers were observed inside pores. The two layers of the construct can be clearly observed in Figure 3.10 B. In order to address changes introduced by DHT treatment and collecting the fibers directly onto foams, fibers were first collected directly onto the aluminum collector and examined. As Figure 3.9 A shows the fibers are flat and straight without any fusion or beading. It is important for a fibrous tissue engineering construct to have no beading. Bead formation decreases the porosity of the fibrous mat and decreases the surface area limiting the cell migration and material transfer [4], which are essential for preparing a 3D tissue equivalent. In the bilayer scaffold fibers showed a similar structure. (Figure 3.9 B) There was no beading and the fibers were flat and straight indicating that the DHT treatment did not cause any deformation in fiber structure supporting the finding in literature [99, 100, 101]. In Figure 3.10 C the pores of the foam underneath can be seen through the fiber layer.
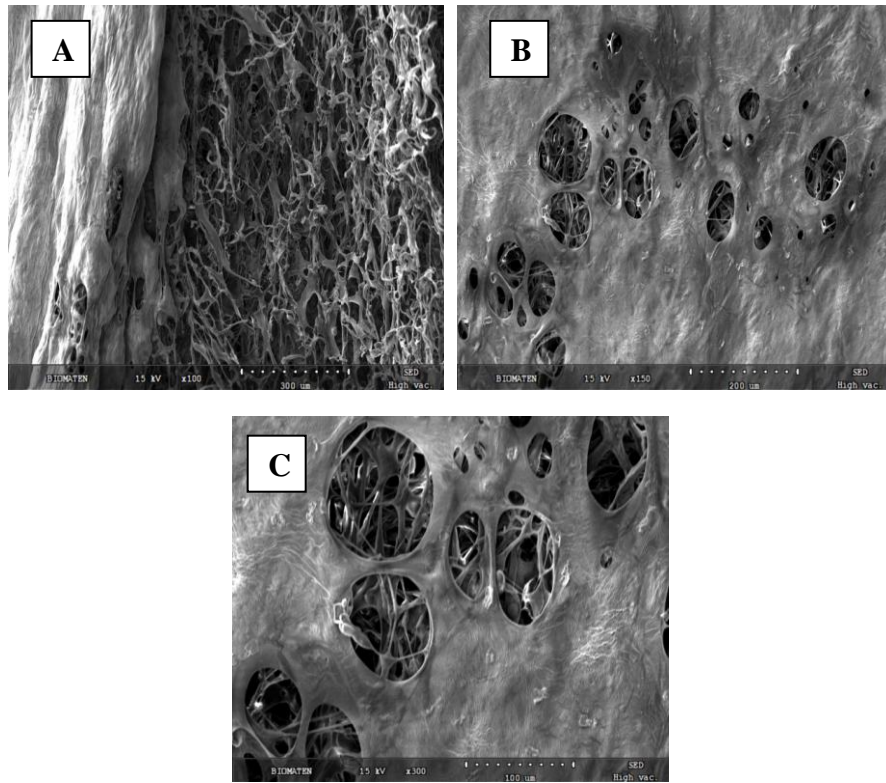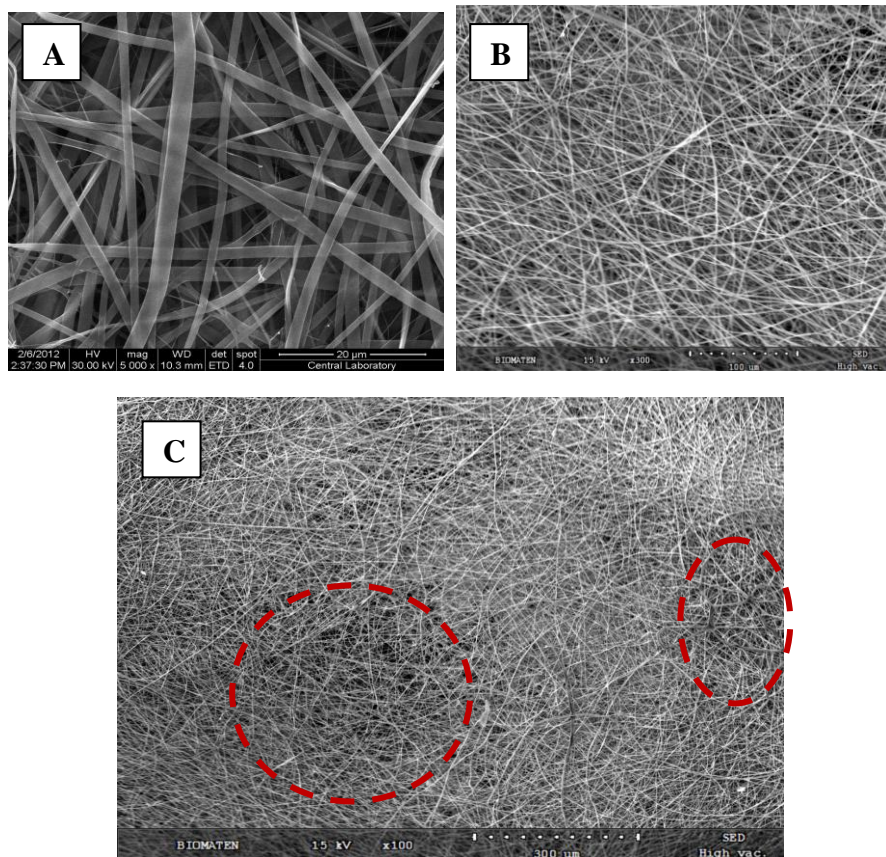
Figure 3. 8. Scanning electron micrograph of XLFs. (A) cross section (x100), (B and C) surface (x150 and x300).
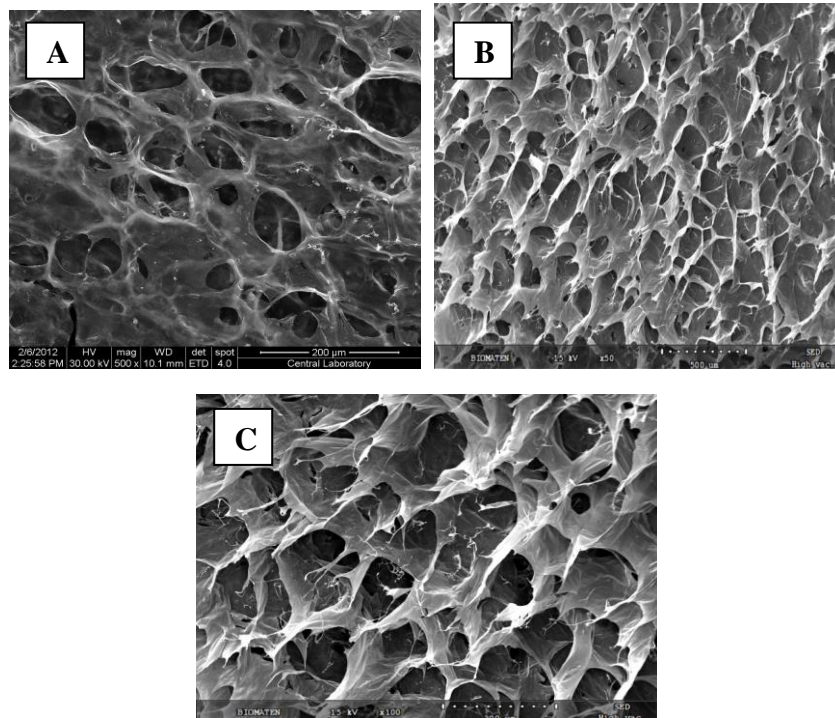
Figure 3. 9. Scanning electron micrograph of CSXLFs. (A) before DHT (x500), (B and C) after DHT (x50 and x100)
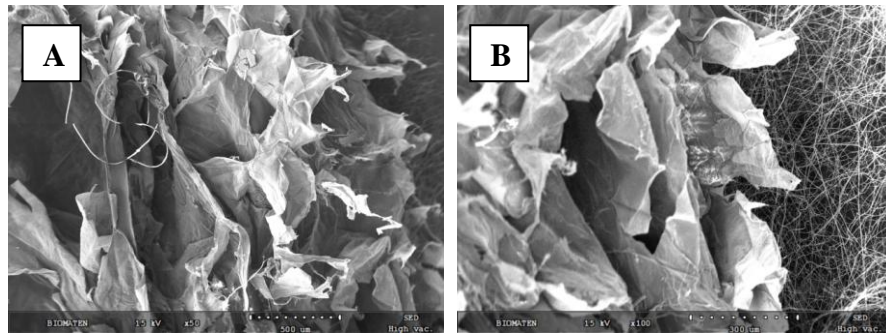
Figure 3. 10. Scanning electron micrographs of Fo-Fi constructs. (A) foam layer, (B) cross section (foam layer on the left and the fibers on the right) (x50, x100).

Figure 3. 11. Scanning electron micrograph of collagen fibrous mats. (A) collected on aluminum collector, (B, C) collected on CSXLFs (x5000, x100) (Pores of the foam underneath are indicated with the circles)

3.2. *In Vitro* Studies

3.2.1.   Cell Attachment and Proliferation on Scaffolds

To examine the cell attachment and proliferation, the scaffolds were seeded with either single cells or co-cultures. The bilayer construct was seeded only with human keratocytes (Fo-Fi HK), only with retinal pigment epithelial cells (Fo-Fi RPE) and with both (Fo-Fi co-culture). Co-culture of CSXLFs were also examined. The results were attained at the end of 1, 7 and 14 days of culture using Alamar

blue assay (Figure 3.12) (calibration curve for absorbance vs cell number is presented in Figure B.1 and B.2 in Appendix B). The cell number in the first day of incubation shows the cell attachment to the scaffolds. The number of keratocytes attached to bilayer scaffolds was significantly higher than that of RPE attached to fiber side of the bilayer scaffold ($p \leq 0.00461$). This is probably due to that the RPE cells were seeded onto the fiber layer of the construct and the fiber layer is much more smooth when compared to the highly porous foam layer. Cells are known to be attached to rough surfaces better [129] and therefore, the 1 hour incubation time might not be enough for epithelial cells to attach to the fibrous layer as much as keratocytes did to foam layer.

As can be seen in the figure, the cell proliferation of all cell-scaffold combinations during week 1 were high, indicating that cells could attach and proliferate on both the scaffolds. However, in the second week (from Day 7 to Day 14) the cell number on all the samples showed a decrease which might suggest that the cells on the scaffolds reached confluency. The decrease or leveling off of the cell numbers on the scaffolds have been reported by literature [116, 117]. It is reported that due to the small sizes of the scaffolds cells reach confluency at the end of one week of culture. In this study the scaffolds were about 2 cm in diameter and about 400 μm thick, which were comparatively smaller than the samples used in other studies in order to mimic the native corneal stroma dimensions [110, 116]. It was observed that retinal pigment epithelial cells were the lowest attached (Day 1), followed by CSXLF with Fo-Fi HK and Fo-Fi co-culture being the highest. They increased by 2-4 fold within the next week and decreased by about 10% in the second week. The decrease in the second week was statistically insignificant ($p>0.05$). Thus, it can be concluded that the cell numbers leveled off during the 2nd week.
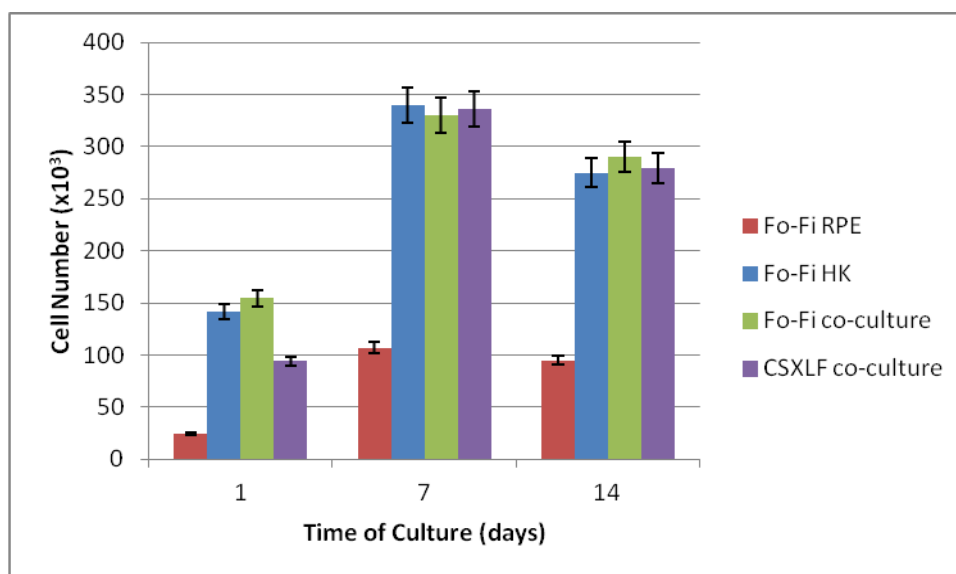
Figure 3. 12. Cell proliferation profile of human keratocytes (HK) and retinal pigment epithelium (RPE) cells on bilayer (Fo-Fi) and single layer (CSXLF) scaffolds.

### 3.2.2. Microscopy of Tissue Engineered Construct

3.2.2.1. FITC-Labeled Phalloidin-DAPI Staining

The attachment of cells to the scaffolds was determined by the cell number count (Figure 3.12). It is also important to observe the cell morphology and distribution on scaffolds before drawing a conclusion about quality of adhesion. In order to achieve that the cytoskeleton of the cells were stained with FITC-labeled phalloidin (green) and their nuclei with DAPI (blue) on days 1, 7 and 14 in the culture medium for both single layer and bilayer constructs (Figures 3.13, and 3.14). Also the same staining procedure was carried out for only keratocyte and only RPE seeded bilayer constructs

on day 14 of culture to show the behavior of the cells without the effect of the second cell type (Figure 3.15). Cell-free bilayer scaffold was stained as a negative control and the keratocyte or RPE seeded cover glasses were stained and used as a positive control (Figure 3.16).

The keratocytes showed the expected fibrous morphology, similar to that observed with the positive control sample (Figure 3.16 B). On day 1 the cells did not seem to have attached to the scaffolds in a specific orientation (Figures 3.13 A and B). At the end of one week, however, the cells lining the pore walls could be clearly seen in both constructs (Figures 3.13 C and D). On day 7 of culture, the co-culture samples were seeded with RPE cells and their micrographs at the end of 14 days of culture are presented in Figures 3.14 A and B. The micrographs of the RPE seeded sides (fiber mat side) of the constructs were taken. Both constructs were well populated with epithelial cells on the surface and no orientation was observed. Similarly on the only keratocyte or only RPE seeded constructs the whole surfaces were covered with cells (Figures 3.15 A, and B, respectively). These results support the cell proliferation assay results, as the cell covered surfaces show that they have reached confluency, which was suggested as the reason behind the leveling off of the cell numbers at the end of the second week of culture.
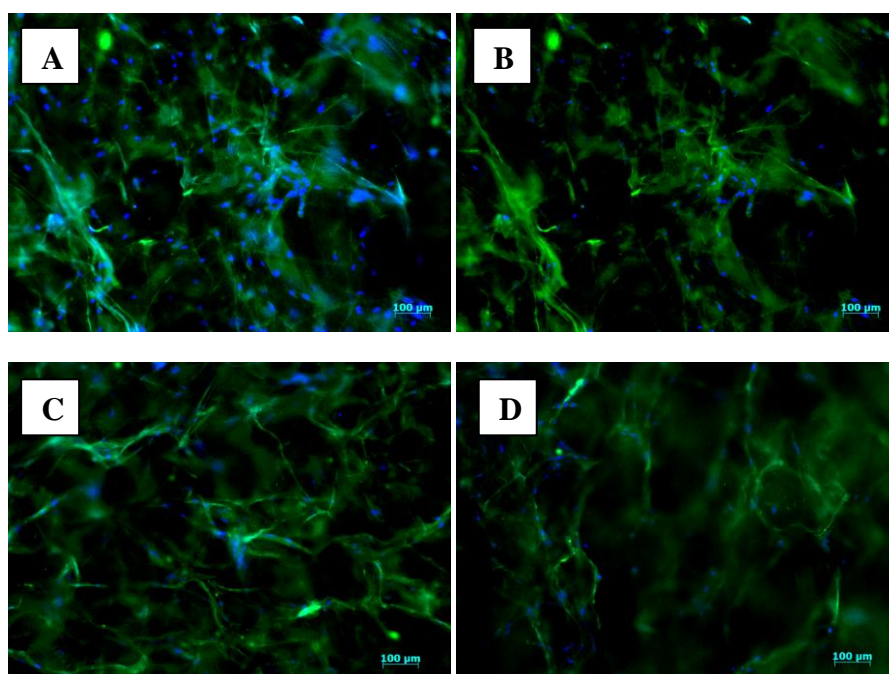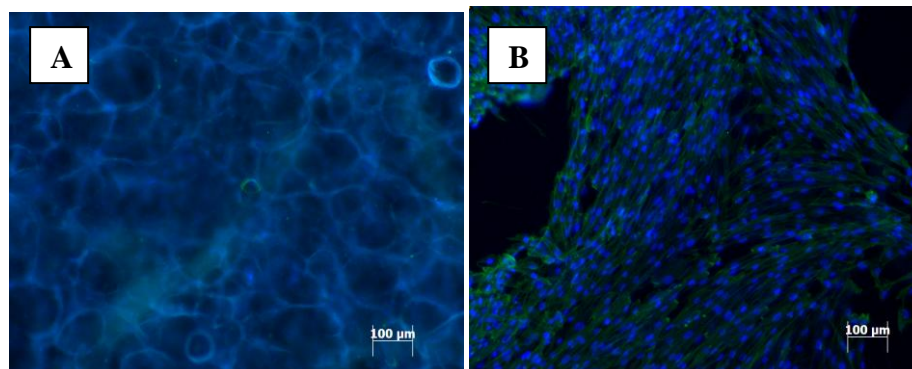

Figure 3. 13. FITC-Phalloidin and DAPI stained foam-fiber and foam constructs. (A, C) Fo-Fi, and (B, D) CSXLF (labeled on 1, and 7 Days of culture, respectively) (magnifications: x10)
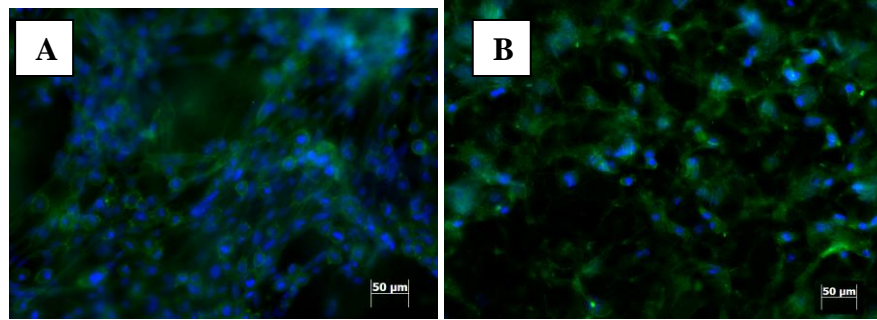
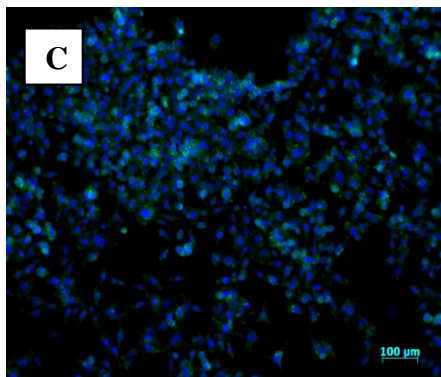**Figure 3. 14**. RPE seeded sides (fiber side) of FITC-Phalloidin and DAPI stained foam-fiber and foam constructs. (A) Fo-Fi, and (B) CSXLF. (labeled on Day 14 of culture) (magnifications: x20)
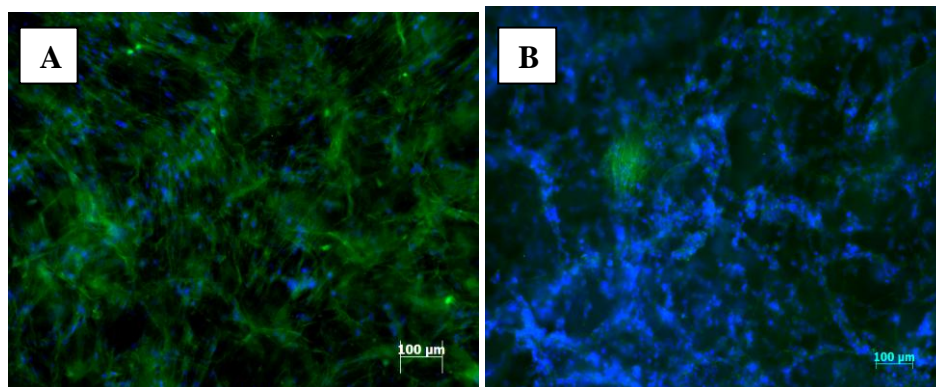
Figure 3. 15. FITC-Phalloidin and DAPI stained Fo-Fi constructs. (A) only keratocyte seeded (foam layer), and (B) only RPE seeded (fiber layer). (labeled on Day 14 of culture) (magnifications: x10)

Figure 3. 16. FITC-Phalloidin and DAPI stained samples. (A) cell-free bilayer scaffold (foam side), (B) only keratocyte seeded cover glass, and (C) only RPE seeded cover glass. (labeled on Day 1 of culture) (magnifications: x10)

3.2.2.2. SEM

The SEM micrographs of only keratocyte and only RPE seeded bilayer constructs were obtained on their 14th day in the culture in order to observe the cell attachment, migration and growth on these constructs. (Figures 3.17-3.19). Figure 3.18 A shows that the keratocytes have populated the foam side of the construct. The porous surface shown in the inset micrograph was totally covered by the cell sheet of human keratocytes, which was previously shown by FITC/DAPI stained fluorescence micrographs (Figure 3.15 A). On the fiber layer of the constructs, however, the cell density seems lower and the fibers on the cells are visible (Figure 3.17 B). The cells were seeded onto the foam layer and since the foam is highly porous, cells move down to the fiber layer and are observed right under the fiber layer. This result is consistent with the immunostaining of Fo-Fi HK 14 day samples for collagen type I deposition, shown in Figure 3.22.
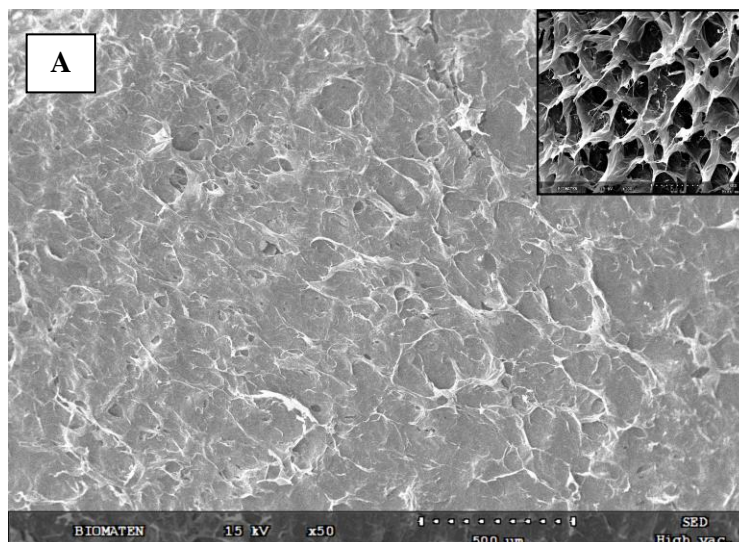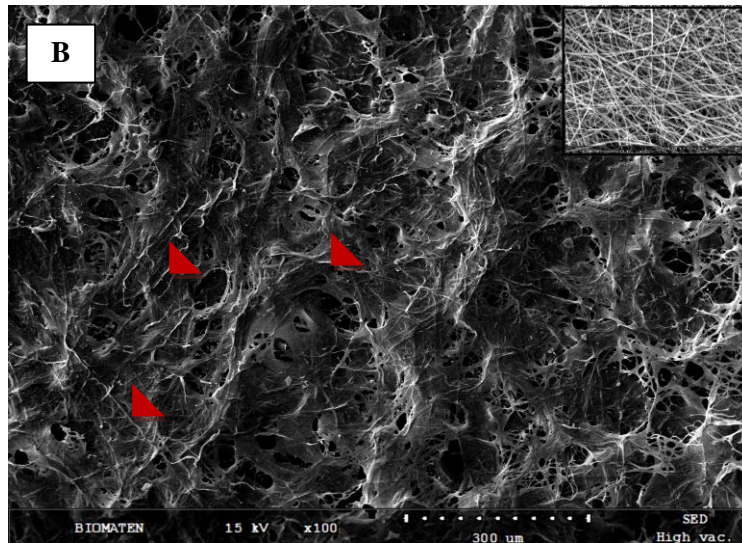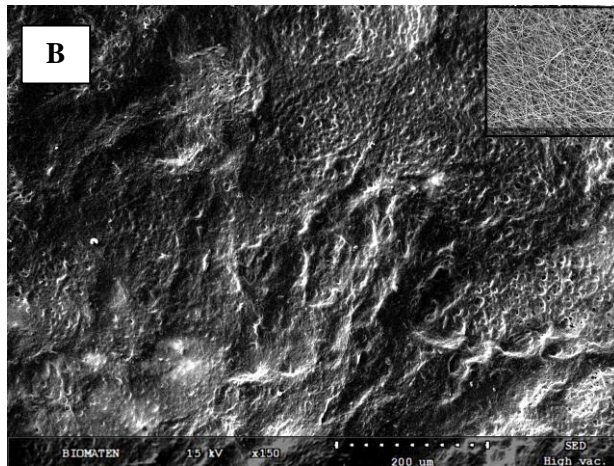
Figure 3. 17. SEM micrographs of human keratocyte seeded (14 day culture) Fo-Fi constructs. (A) foam (x50), and (B) fiber surface (x100). (inset: cell-free constructs from Figure 3.8 and Figure 3.9, respectively). (Red arrows indicate the fibers).

RPE cells were seeded onto the fiber layer of the scaffolds and the cells were observed on the fiber layer as shown in Figures 3.18 and 3.19. The foam part of the construct shows the porous structure similar to the cell free constructs (Figure 3.18 A inset) indicating that the cells did not pass through the fiber layer and migrate down to the foam layer (Figure 3.18 A). On the other hand, the fiber layer was covered with RPEs, which formed a cell sheet over the whole scaffold surface. The cross sections of these constructs seeded with RPEs also show the cell sheet formation on the fiber layer (Figures 3.19 A and B). This is consistent with the FITC/DAPI staining (Figure 3.15 B) results. Also, the highly porous and non-populated foam layer could be more clearly observed.
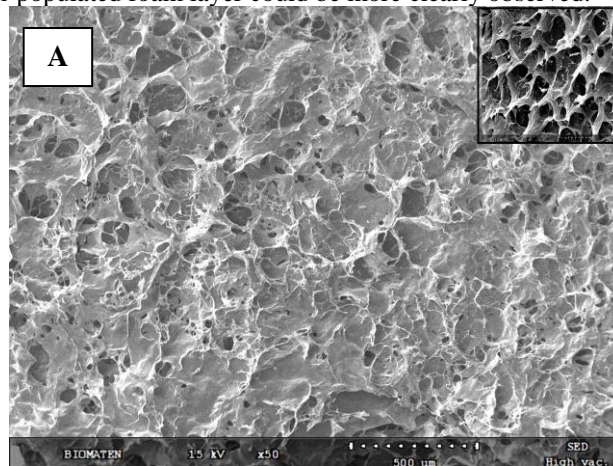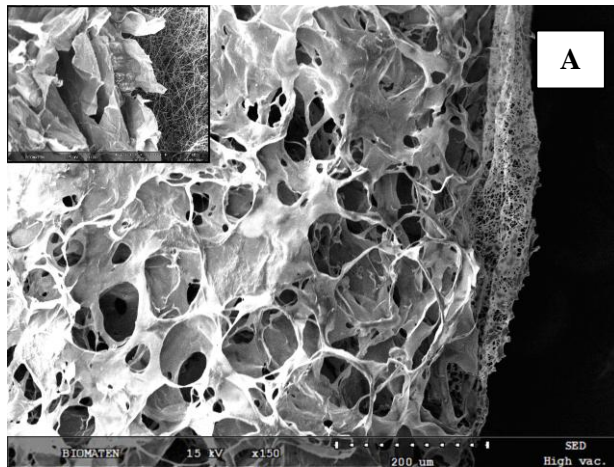
Figure 3. 18. SEM micrographs of RPE seeded (14 day culture) Fo-Fi constructs, (A) foam (x50), and (B) fiber surface (x150). (inset: cell-free constructs, Figures 3.8 and 3.9 respectively).
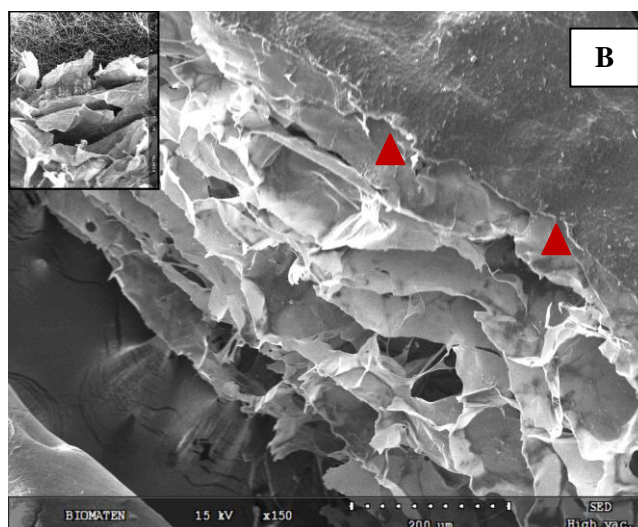
Figure 3. 19. SEM of cross sections of RPE seeded (14 day culture) Fo-Fi constructs, (A) foam, and (B) fiber surface on top. (x150) (inset: cell-free construct, Figure 3.10 B). (red arrows indicate the RPE sheet on the fiber layer).

3.2.3. Immunostaining

3.2.3.1. Collagen Type I Staining

The collagen type I deposition on the scaffolds were examined by immunostaining of the constructs against human collagen type I (Figures 3.20, 3.21, and 3.22). All the samples were stained on Days 1, 7 and 14 of culture and the effect of the co-culture on collagen deposition and the effect of fiber layer on cell penetration were studied. It is important for isolated cells to show that they did not lose their characteristic functions as they were passaged. Collagen type I is the main ECM protein synthesized by the stromal keratocytes, thus its deposition would indicate that the cells did not lose their phenotype and did not differentiate into another cell type. It is also important to show the native ECM secretion by the cells, indicating the construction of the neo-tissue as a result of healthy growth of cells.

FITC-phalloidin stains the actin fibers in the cell cytoskeleton to green and gives information about the cell morphology and penetration into constructs. The deposited collagen was represented red in color because Alexafluor532 labeled anti-mouse Ig antibody was used as the fluorescent label. Since collagen has autofluorescence at almost every wavelength, the constructs always had a background signal. The distinction between the dyes and the autofluorescence was achieved by overlaying the signals collected by the two stains. The scaffold gives fluorescence at both wavelengths, thus, when the two micrographs were overlaid, it appeared yellow which can be easily differentiated from cells (green) and the deposited collagen (red dots represented in black circles in Figure 3.22). The examination of the co-cultured scaffolds was made by scanning from both upper surface (fiber layer on top) and lower surface (foam layer on top). The expectation was to have the RPE cells on top of the fibers and keratocytes in the foam layer, which were separated by the fiber layer, that did not prevent their contact and material transfer. The cross section views of the constructs show how deep the cells penetrated into the constructs which is an indication of the success of the fiber layer in preventing the intermixing of the two cell types.
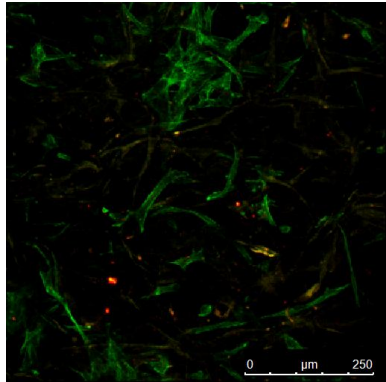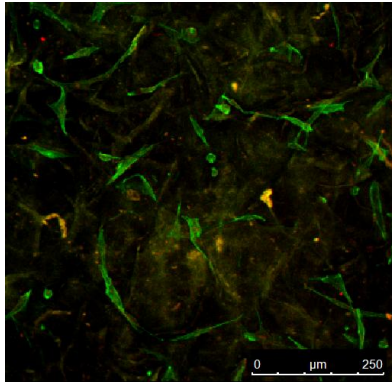
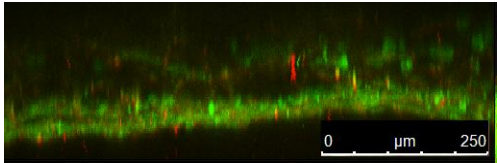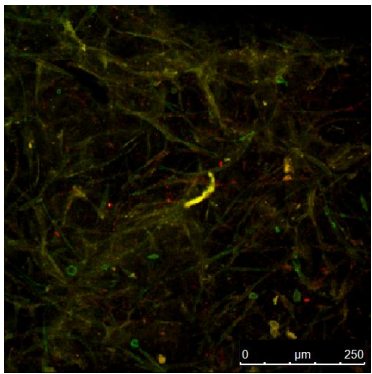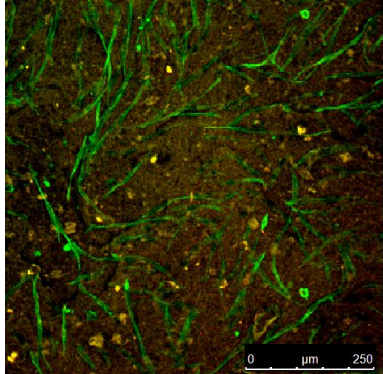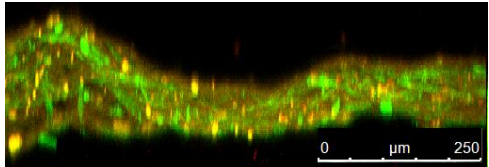Figure 3.20 shows that the only keratocyte seeded bilayer scaffolds on Days 1 and 7 of incubation had almost no collagen deposited. Similarly the keratocyte seeded single layer constructs had no collagen deposition during the same time period (Figure 3.21). On Day 14 of the culture the co-cultured

41

constructs start deposition of collagen (Figure 3.22). However, on Day 14 there was no ECM secretion on the constructs seeded with only keratocytes. This indicates that the presence of the epithelial cell layer induces collagen type I secretion by keratocytes; this observation is also supported by the literature [118].

When the cell penetration on Days 1 and 7 was studied, the bilayer scaffolds showed that the cells migrated down to the fiber layer; however, cells on the foam layer were also observed (Figure 3.20).

The single layer scaffolds (only foam) also had cells both at the bottom (opposite side of cell seeding) and at the top (side of cell seeding). Results of day 7 show that the cells proliferated on the bottom of the scaffold almost covering the whole surface (Figure 3.21). This indicates that the cells moved within the foam and reached the opposite surface. The cross sections of bilayer and single layer constructs on day 7 also show that the bilayer scaffolds had cell growth mainly in the middle part of the scaffolds unlike the single layered ones having the major cell growth at the bottom surface. This indicates that the fiber layer prevented further cell migration to the bottom surface (since keratocytes were seeded onto the foam layer, until RPE seeding the fiber layer remains as the bottom layer) of the bilayer constructs.

On day 14, the co-cultured bilayer scaffold had its foam surface covered with keratocytes and the fiber layer with RPE cells (Figure 3.22). The RPE cells can be easily differentiated from keratocytes as they have a very distinct morphology: (keratocytes have fibrous morphology, and the RPEs have a round morphology). The presence of the orange colored scaffold right beneath the epithelial cells also proves that the keratocytes seeded from the opposite direction did not populate the fiber layer. The CSXLFs, however, had fewer cells on the keratocyte seeded surface as mentioned above, and the RPE cells were, therefore, seeded onto the keratocyte layer formed on the foam. This can be seen clearly in the top view of the scaffolds (Figure 3.22) as the scaffolds are barely seen through the RPEs. The only keratocyte seeded bilayer scaffolds had the major cell growth at the cell seeding surface and the mid part of the scaffold. Cells on the fiber layer were also observed, supporting the presence of cells on that layer on day 7 also. This result is also consistent with the SEM images of keratocyte seeded bilayer constructs as they showed a major cell growth at the foam side along with cells penetrated to the fiber layer, which are lower in number (Figures 3.18 A, and B).
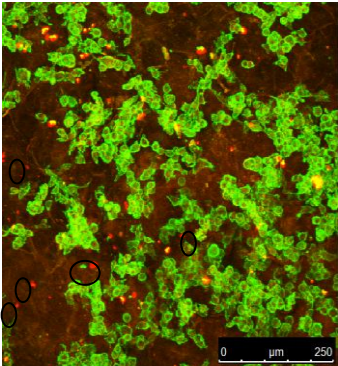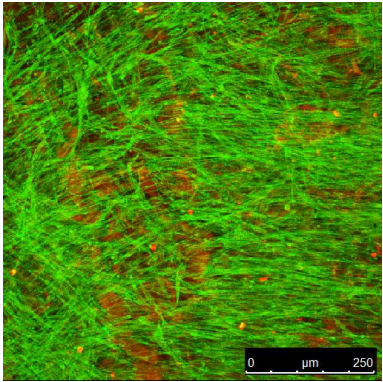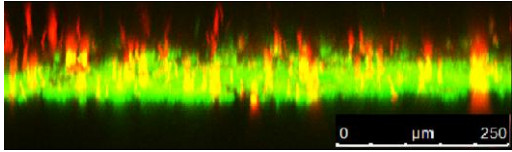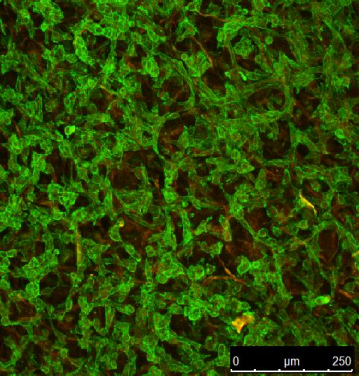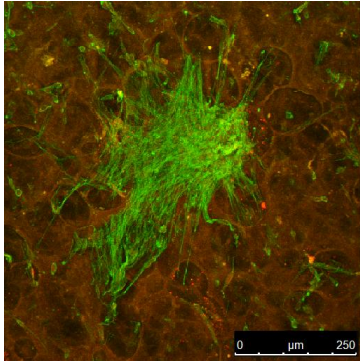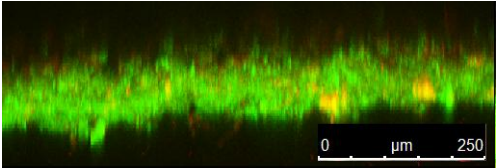
Culture Duration (days)	Fo-Fi HK		
	Top (fiber)	Bottom (foam)	Cross section* (fiber layer on top)
1			
7			

Figure 3. 20. Collagen type I deposition on the only keratocyte seeded bilayer (Fo-Fi HK) constructs. *Sections were about 200-250 μm thick.

	CSXLF HK		
Culture (days)	Top*	Bottom	Cross section**
1			
7			
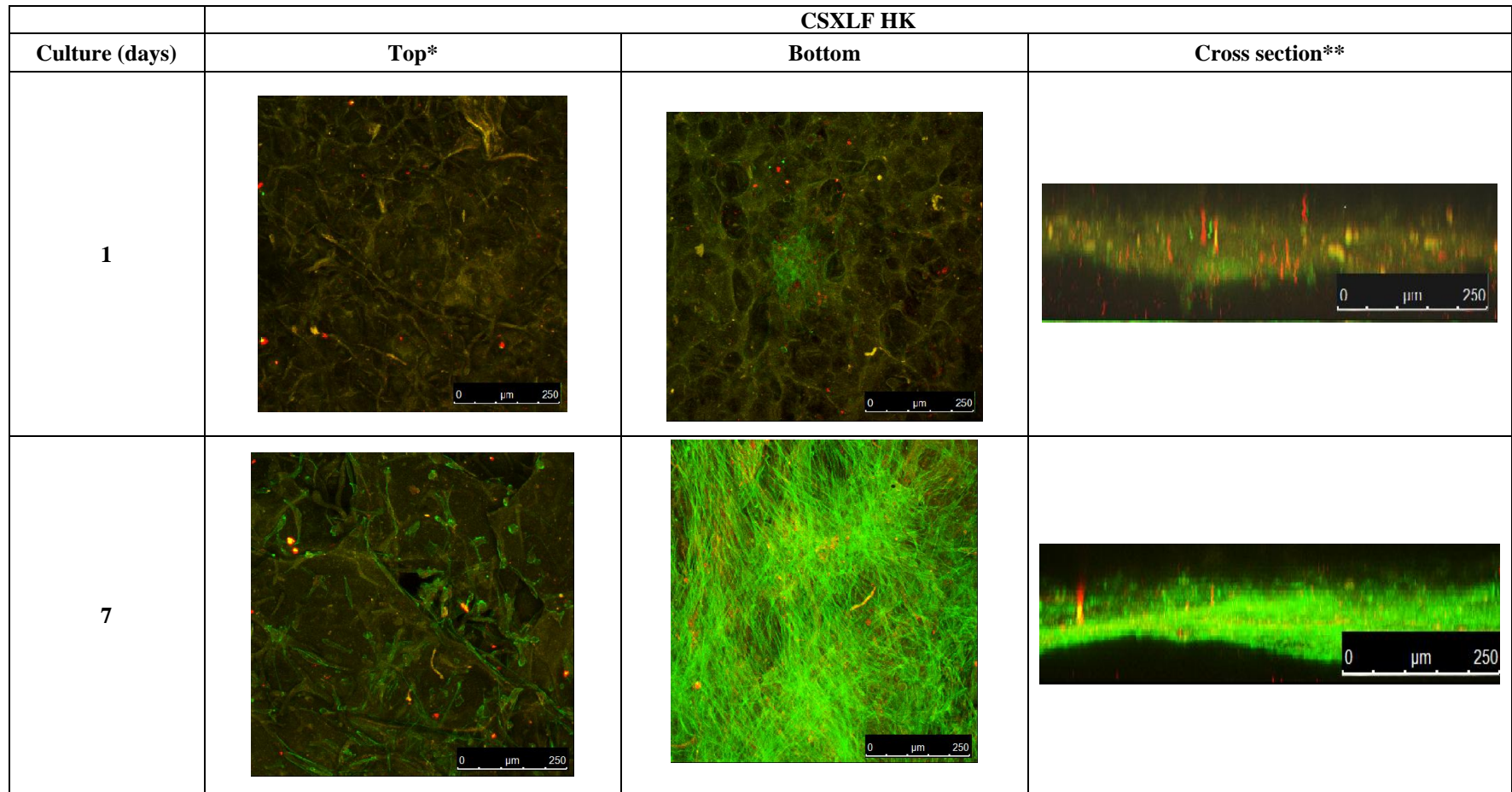
Figure 3. 21. Collagen type I deposition on the only keratocyte seeded single layer scaffolds (CSXLF HK). *Top side of CSXLF samples was the side of cell seeding. ** Sections were about 200-250 μm thick.

Construct Type*	Top	Bottom	Cross section**
Fo-Fi Co-culture	(fiber, RPE seeded)	(foam, keratocyte seeded)	(fiber layer on top)
CSXLF Co-culture	(RPE seeded side of the foam)	(keratocyte seeded side of the foam)	(RPE seeded side on top)

Fo-Fi HK	 **(fiber, not seeded)**	 **(foam, keratocyte seeded)**	 **(fiber layer on top)**
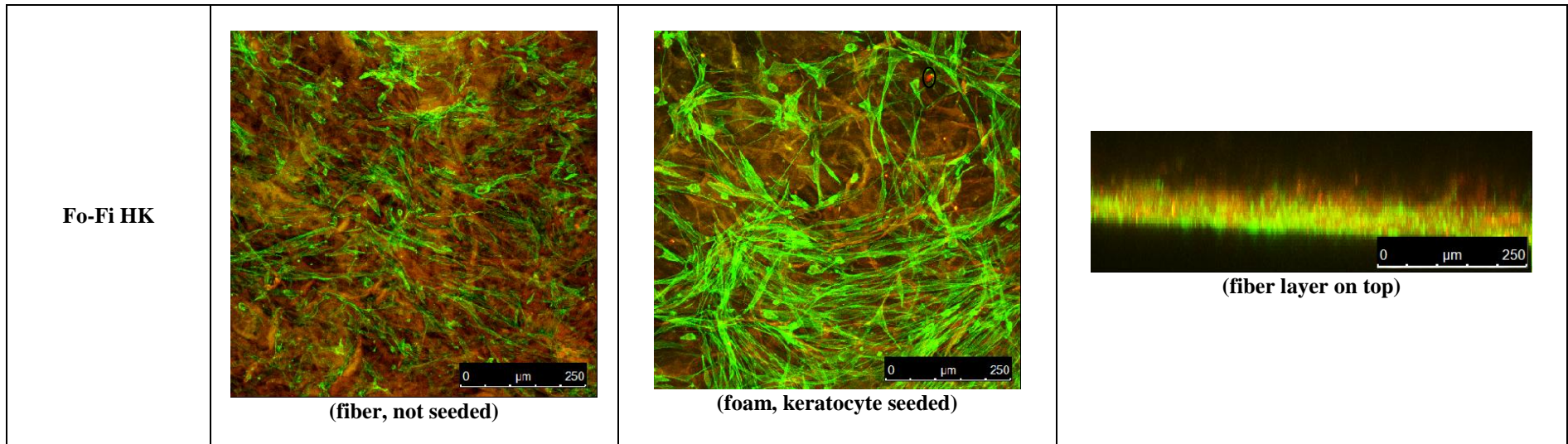
Figure 3. 22. Collagen type I deposition on the co-cultured single layer and bilayer scaffolds. (Black circles indicate the deposited collagen type I) *All constructs were examined on Day 14 of culture. ** Sections were about 200-250 µm thick.

3.2.4. Light Transmittance and Transparency of Scaffolds

The 3 different cell seeded constructs were tested for their light transmittance on Day 1, 15, 31 (Figures 3.23 A, B and C). All three samples showed a similar pattern through the scanned wavelength range, starting with a lower transmittance until 300 nm and gradually increasing at higher wavelengths.

On the first day of incubation the light transmittance was as expected (Figure 3.23 A). As mentioned in Section 3.1.2.7., normal human cornea has lower transmittance in UV-B and C regions like the spectra presented in this study. The results for Fo-Fi co-culture and Fo-Fi HK samples were very close as expected since the co-cultured scaffolds were seeded with the epithelial cells on day 7 of culture. Thus, both first day samples were seeded only with human keratocytes. The light transmittance of both was in the desired range (close to 85%) in the visible region. Similarly, the CSXLF co-culture samples were seeded only with keratocytes at that time point. These single layer scaffolds, however, had a slightly lower light transmission (about 80%) than the bilayer scaffold. This is consistent with the results for cell-free scaffolds as the former had a higher light transmittance than the latter (Figure 3.6). At the end of 15 days, the light transmittance of the scaffolds were close to that of day 1 with a slight decrease in the co-cultured bilayer construct. This decrease was probably caused by the thickening of the scaffolds with cell growth and their ECM production (Figure 3.22). On day 31 the light transmittance of co-cultured bilayer construct increased by one percent (82 to 83%) and that of single layer scaffold decreased by 5% (82 to 77%). The Fo-Fi HK samples, however, had a rather stable transmittance over the last two weeks of culture. Overall, the CSXLF co-culture constructs showed a lower transparency through the course of the one month culture preiod. The constructs with the fiber layer, co-cultured or keratocyte seeded, transmitted more visible light suggesting that these scaffolds are better in terms of transparency.

In the literature various corneal replacements were tested for their transparency and many of collagen based scaffolds had inferior light transmittance in the visible light region. In the study of Vrana et al., patterned and unpatterned films, and soluble and insoluble foams were scanned between 250-700 nm. The scaffolds showed a similar pattern as the transmittance was lower up to 300 nm, followed by an increase in visible light region. Although there was an increase over 7 days of incubation, the overall transparencies at best were 40% for the films and 5% for soluble foams. In another study, Orwin and colleagues [119] studied reconstruction of corneal stroma with DHT crosslinked collagen based sponges (with and without chondroitin sulfate incorporation) and gels and tested their transparencies on day 21 of corneal keratocyte culture. The light transmittance (at 700 nm) of sponges without chondroitin sulfate was about 33%, whereas the gels prepared as control showed a significantly lower transmittance (5%). The incorporation of chondroitin sulfate increased the transmittance to approximately 50%.

Superior transparencies were also achieved in other studies [120, 121]. Kadakia *et al.,* designed a hybrid scaffold of collagen and polyethylene glycol diacrylate (PEGDA). The construct had the core made up of PEGDA and the skirt comprised of collagen-PEGDA mixture. Although the core part had a light transmittance of about 90% in the visible range, it was around 70% in the UV range. Moreover, it was shown that the skirt had a more opaque structure due to the introduction of collagen into the structure. This supports the lower light transmittance of the scaffolds designed in this study as they were collagen based and unorganized collagen presence causes light to scatter. This is mainly due to the random arrangement of collagen fibrils [105]. This can explain the relatively lower (85% with respect to 99% of native) transmittance of the constructs prepared in this study since the reconstruction of stroma and epithelium layers of the cornea was achieved with foams, comprised of collagen fibers with random distribution, and randomly arranged collagen electrospun fibers. It is, however, expected to improve significantly in time as the cells will secrete their own ECM and reorganize the layers.
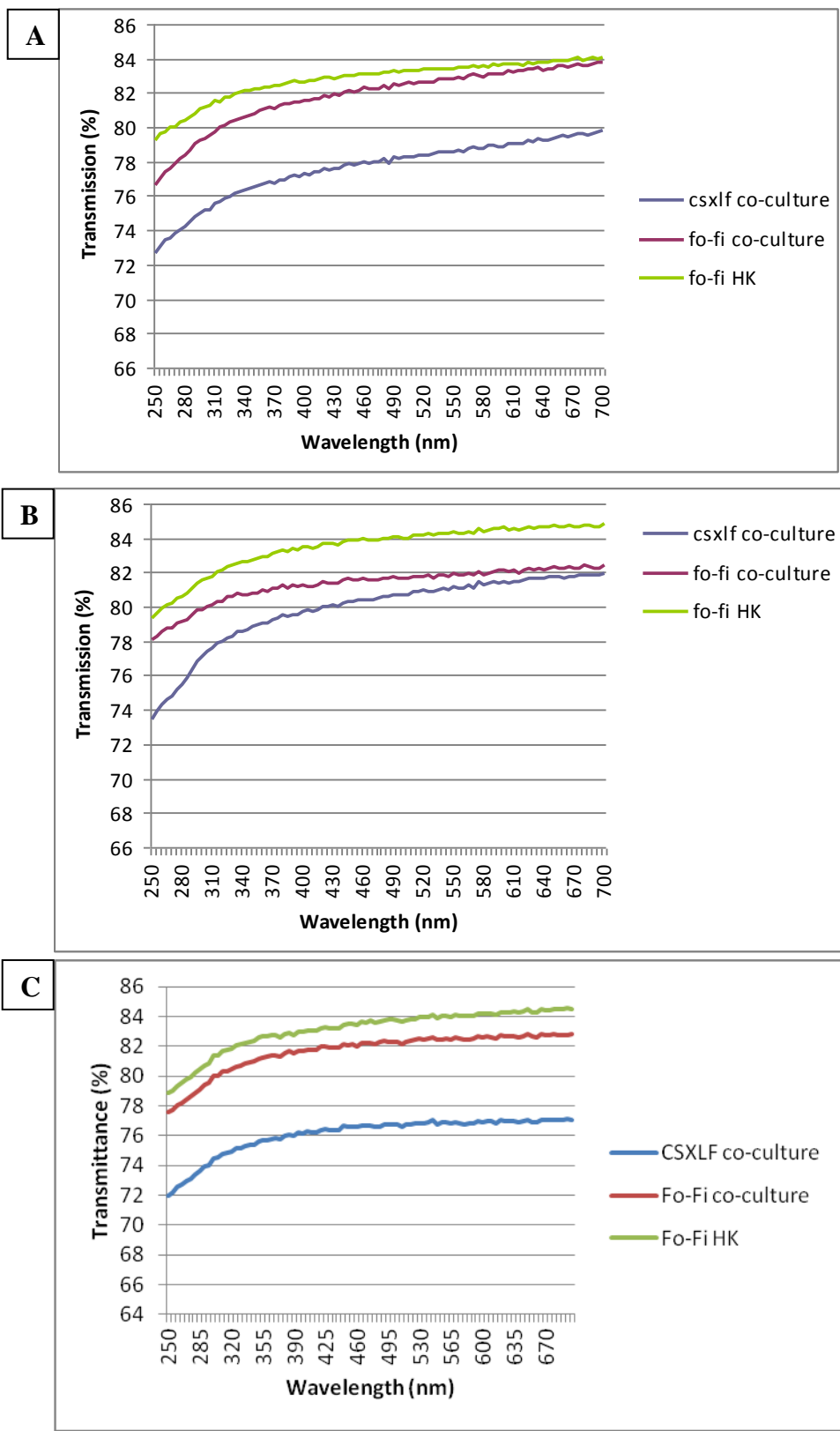
Figure 3. 23. Light transmittance of constructs on Days (A) 1, (B) 15, and (C) 31

3.2.5. Suturability Testing

The performance of the bilayer construct during suturing process was tested with a sample in its 31st day of culture using 6.0 prolene suture with cutting needle. The construct was placed on top of the round, padded surface covered with gauze. Suturing was carried out to completely fix the construct on the pad. The sample showed good resistance and no major tears formed during the process (Figure 3.20).

Figure 3. 24. Proof of the suturability of the bilayer co-cultured construct. This sample was cultured for 31 days.

CHAPTER 4

CONCLUSION AND FUTURE STUDIES

Corneal blindness is the second most common cause of blindness in the world and can result from any physical or chemical impacts, infections and inherited diseases.

In this study a novel, bilayer scaffold was constructed of collagen type I and chondroitin sulfate. The bottom layer of the bilayer was intended to construct the stroma layer and the top layer to mimic Bowman's membrane.

Current study uniquely mimics the two upper layers of the cornea. As opposed to other studies a basement membrane was introduced into the structure for the epithelial cells to proliferate and this helped separate the cells but allowed transport. So a Bowman's membrane function was performed without actually having a tight membrane. The ECM secretion in the co-culture showed that the approach was successful. The suturability of this transparent cornea only after 4 weeks shortens the period patient waits to gain his vision back. This is a very good achievement that has to be tested *in vivo*. These studies should be carried out with rabbit using rabbit cornea epithelial cells and rabbit keratocytes as a preparation for a clinical test using human cells. In future studies the mechanical properties of the constructs should also be determined.

REFERENCES

1. Griffith M, Fagerholm P, Lagali N, Latorre M, Hackett J, Sheardown H. Regenerative medicine in the cornea. In: Principles of Regenerative Medicine. 2nd ed. 2011; 911-924.

2. Randall VT. Cornea. In: Lanza RP, Langer RS, Vacanti JP, editors. Principles of Tissue Engineering. 2nd ed. Academic Press, 2000; 471-491.

3. Lanza RP, Langer RS, Vacanti J. Corneal-Tissue Replacement. In: Lanza RP, Langer RS, Vacanti JP, editors. Principles of Tissue Engineering. 3rd ed. Amsterdam; Boston: Elsevier / Academic Press, 2007; 1025-1049.

4. Ruberti JW, Zieske JD. Prelude to corneal tissue engineering – Gaining control of collagen organization. Prog Retin Eye Res 2008; 27:549-577.

5. Sheardown H, Griffith M. Regenerative Medicine in the Cornea. Principles of Regenerative Medicine. 2nd ed. San Diego: Academic Press, 2008; 1060-1071.

6. Randall VT. Cornea. In: Lanza RP, Langer RS, Chick W, editors. Principles of Tissue Engineering. 1st ed. Academic Press, 1997; 383-402.

7. Bohnke M, Masters BR. Confocal microscopy of the cornea. Prog Retin Eye Res. 1999; 18:553-628.

8. Nagy Z, Hiscott P, Seitz B, Shlötzer-Schrehardt U, Simon M Jr, Süveges I, Naumann GO. Ultraviolet-B enhances corneal stromal response to 193-nm excimer laser treatment. Ophthalmology. 1997; 104:375–380.

9. Kolozsvari L, Nogradi A, Hopp B, Bor Z. UV absorbance of the human cornea in the 240- to 400-nm range. Invest Ophthalmol Vis Sci 2002; 43:2165-2168.

10. Meek KM, Boote C. The organization of collagen in the corneal stroma. Exp Eye Res 2004; 78:503-512.

11. Maurice DM. The structure and transparency of the cornea. J Physiol 1957; 136:263–286.

12. Miller GE. Artificial and replacement cornea. In: Sensory Organ Replacement and Repair. 1st ed. California: Morgan & Claypool, 2006; 48-49.

13. Abrams GA, Schaus SS, Goodman SL, Nealey PF, Murphy CJ. Nanoscale Topography of the Corneal Epithelial Basement Membrane and Descemet's Membrane of the Human. Cornea. 2000; 19:57-64.

14. Meek KM, Fullwood NJ, Corneal collagens: Corneal and scleral collagens. A microscopist's perspective. Micron, 2001; 32, 261-272.

15 Kaufman HE, Wright KW, Ryan SJ. Cornea. Color atlas of ophthalmic surgery. Corneal and refractive surgery. Philedelphia: Lippincott, 1992; 2-11.

16. Coster D. The cornea and inflammation: diagnosing the red eye. In: Cornea: Fundamentals of Clinical Ophthalmology Series. London: BMJ Books, 2002; 35-41.

17. Whitcher J, Srinivasan M, Upadhyay MP. Corneal blindness: a global perspective. Bulletin of the World Health Organization, 2001; 79:214–221.

18. Chirila TV, Hicks CR, Dalton PD, Vijayasekaran S, Lou X, Hong Y, Clayton AB, Ziegelaar BW, Fitton JH, Platten S, Crawford GJ, Constable IJ. Artificial cornea. Progress in Polymer Science 1998;23:447-473.

19. Cursiefen C, Kruse EF, New Aspects of Angiogenesis in the Cornea. In: Reinhard T, Larkin DFP, editors. Essentials in Opthalmology: Cornea and External Eye Disease. 1st ed. 2006; 83-98.

20. Chalupa E, Swarbrick HA, Holden BA, Sjöstrand J. Severe corneal infections associated with contact lens wear. Ophthalmology. 1987; 94(1):17-22.

21. Adamis PA, Filatov V, Tripathi BJ, Tripathi RA. Fuchs' endothelial dystrophy of the cornea. Survey of Ophthalmology. 1993; 38:149-168.

22. Klausner EA, Peer D, Chapman RL, Multack RF, Andurkar SV. Corneal gene therapy. J Controlled Release 2007;124:107-133.

23. Claesson M, Armitage WJ, Fagerholm P, Stenevi U, Visual outcome in

corneal grafts:a preliminary analysis of Swedish corneal transplant register, Br J Ophthalmol, 1997; 86:174-180.

24. Claesson M, Armitage WJ, Fagerholm P, Stenevi U. Visual outcome in corneal grafts: a preliminary analysis of the Swedish Corneal Transplant Register. Br J Ophthalmol 2002;86:174-180.

25. Girard LJ. Girard keratoprosthesis with flexible skirt 28 years experience. Refract Corneal Surg. 1993; 9:194-195.

26. Lanza RP, Langer RS, Vacanti J. Introduction to Tissue Engineering. Principles of tissue engineering. 3rd ed. Amsterdam ; Boston: Elsevier/Academic Press, 2007; 1-33.

27. Ikada Y. Scope of Tissue Engineering. Tissue engineering: Fundamentals and applications. 1st ed. Amsterdam; Boston: Academic Press/Elsevier, 2006; 1-26.

28. Meyer U. General and Ethical Aspects. In: Meyer U, Meyer T, Handschel J, Wiesmann HP, editors. Fundamentals of tissue engineering and regenerative medicine. 1st ed. New York: Springer, 2008; 5-13.

29. Khademhosseini A, Langer R, Borenstein J, Vacanti JP. Microscale technologies for tissue engineering and biology. PNAS. 2006; 8:2480-2487.

30. Web site of National University Health Sytem. Illustration retrieved from http://www.nuhs.edu.sg/research/programmatic-research/som-registered-programmes/nus-tissue-engineering-programme.html

31. Lanza RP, Langer RS, Vacanti J. Stem Cells. In: Lanza RP, Langer RS, Vacanti JP, editors. Principles of Tissue Engineering. 3rd ed. Amsterdam; Boston: Elsevier / Academic Press, 2007; 419-459.

32. Ikada, Y. Cell Expansion and Differentiation. Tissue engineering: Fundamentals and Applications. 1st ed. Boston: Elsevier / Academic Press, 2006; 41-51.

33. Risbud M. Tissue engineering: implications in the treatment of organ and tissue defects. Biogerontology. 2001; 2:117-125.

34. Stock UA, Vacanti JP. Tissue engineering: current state and prospects. Ann Rev Med. 2001; 52:143–151.

35. Burdick JA, Anseth KS. Photoencapsulation of osteoblasts in injectable RGD-modified PEG hydrogels for bone tissue engineering. Biomaterials. 2002;23:4315-4323.

36. Ma L, Gao C, Mao Z, Zhou J, Shen J, Hu X, Han C. Collagen/chitosan porous scaffolds with improved biostability for skin tissue engineering. Biomaterials. 2003; 24:4833-41.

37. Carrier RL, Papadaki M, Rupnick M, Schoen FJ, Bursac N, Langer R, Freed LE,Vunjak-Novakovic G. Cardiac tissue engineering: cell seeding, cultivation parameters, and tissue construct characterization. Biotechnol Bioeng. 1999; 64:580-9.

38. Nettles DL, Elder SH, Gilbert JA. Potential use of chitosan as a cell scaffold material for cartilage tissue engineering. Tissue Eng. 2002; 8:1009-16.

39. Vrana NE, Builles N, Justin V, Bednarz J, Pellegrini G, Ferrari B, Damour O, Hulmes DJ, Hasirci V. Development of a reconstructed cornea from collagen-chondroitin sulfate foams and human cell cultures. Invest Ophthalmol Vis Sci. 2008; 49:5325-31. doi: 10.1167/iovs.07-1599.

40. Griffith LG, Naughton G. Tissue engineering--current challenges and expanding opportunities. Science. 2002; 295:1009-14.

41. Liu Y, Ren L, Yao H, Wang Y. Collagen films with suitable physical properties and biocompatibility for corneal tissue engineering prepared by ion leaching technique. Materials Letters. 2012; 87:1–4.

42. Koizumi N, Inatomi T, Quantock AJ, Fullwood NJ, Dota A, Kinoshita S. Amniotic membrane as a substrate for cultivating limbal corneal epithelial cells for autologous transplantation in rabbits. Cornea. 2000; 19:65-71.

43. Alaminos M, Del Carmen Sánchez-Quevedo M, Muñoz-Avila JI, Serrano D, Medialdea S, Carreras I, Campos A. Construction of a complete rabbit cornea substitute using a fibrin-agarose scaffold. Invest Ophthalmol Vis Sci. 2006; 47:3311-7.

44. Griffith M, Osborne R, Munger R, Xiong X, Doillon CJ, Laycock NL, Hakim M, Song Y, Watsky MA. Functional human corneal equivalents constructed from cell lines. Science. 1999; 286:2169-72.

45. Reichl S, Döhring S, Bednarz J, Müller-Goymann CC. Human cornea construct HCC-an alternative for in vitro permeation studies? A comparison with human donor corneas. Eur J Pharm Biopharm. 2005; 60:305-8.

46. Liu W, Merrett K, Griffith M, Fagerholm P, Dravida S, Heyne B, Scaiano JC, Watsky MA, Shinozaki N, Lagali N, Munger R, Li F. Recombinant human collagen for tissue engineered corneal substitutes. Biomaterials. 2008; 29:1147-58.

47. Wang S, Liu W, Han B, Yang L. Study on a hydroxypropyl chitosan–gelatin based scaffold for corneal stroma tissue engineering. Applied Surface Science. 2009; 255:8701-5.

48. Carrier P, Deschambeault A, Audet C, Talbot M, Gauvin R, Giasson CJ, Auger FA, Guérin SL, Germain L. Impact of cell source on human cornea reconstructed by tissue engineering. Invest Ophthalmol Vis Sci. 2009; 50:2645-52. doi: 10.1167/iovs.08-2001.

49. Kobayashi H, Kato M, Taguchi T, Ikoma T, Miyashita H, Shimmura S, Tsubota K, Tanaka J. Collagen immobilized PVA hydrogel-hydroxyapatite composites prepared by kneading methods as a material for peripheral cuff of artificial cornea. Materials Science and Engineering:C. 2004; 24:729–735.

50. Mimura T, Amano S, Yokoo S, Uchida S, Yamagami S, Usui T, Kimura Y, Tabata Y. Tissue engineering of corneal stroma with rabbit fibroblast precursors and gelatin hydrogels. Mol Vis. 2008; 14:1819-28.

51. Zhang YQ, Zhang WJ, Liu W, Hu XJ, Zhou GD, Cui L, Cao Y. Tissue engineering of corneal stromal layer with dermal fibroblasts: phenotypic and functional switch of differentiated cells in cornea. Tissue Eng Part A. 2008;14:295-303. doi: 10.1089/tea.2007.0200.

52. Engelke M, Zorn-Kruppa M, Gabel D, Reisinger K, Rusche B, Mewes KR. A human hemi-cornea model for eye irritation testing: Quality control of production, reliability and predictive capacity. Toxicol In Vitro. 2013; 27:458-68. doi: 10.1016/j.tiv.2012.07.011.

53. Flanagan TC, Wilkins B, Black A, Jockenhoevel S, Smith TJ, Pandit AS. A collagen-glycosaminoglycan co-culture model for heart valve tissue engineering applications. Biomaterials. 2006; 27:2233-46.

54. Choong SN, Hutmacher WD, Triffitt JT. Co-culture of Bone Marrow Fibroblasts and Endothelial Cells on Modified Polycaprolactone Substrates for Enhanced Potentials in Bone Tissue Engineering Tissue Engineering. 2006; 12:2521-2531. doi:10.1089/ten.2006.12.2521.

55. Ikada Y. Basic Technologies Developed for Tissue Engineering. In: Tissue Engineering: Fundamentals And Applications. 1st ed. Amsterdam; Boston: Academic Press/Elsevier, 2006; 328-338.

56. Dai N, Yeh M, Liu DD, Adams EF, Chiang C, Yen C, Shih C, Sytwu H, Chen T, Wang H, Williamson MR, Coombes AGA. A co-cultured skin model based on cell support membranes. Biochem Biophys Res Commun 2005; 329:905-908.

57. Acarturk TO, Adipose tissue engineering In: Meyer U, Meyer T, Handschel J, Wiesmann HP, editors. Fundamentals of tissue engineering and regenerative medicine. 1st ed. New York: Springer, 2008; 289-307.

58. Berthiaume F, Tilles AW, Toner M, Yarmush L, Chan C.Adjunct and Temporary Liver Support. In: Francis JP, Mikos AG, Bronzino DJ. Tissue engineering. London: CRC; Taylor & Francis, 2007; 30-1-30-14.

59. Hendriks J, Riesle J, van Blitterswijk CA. Co-culture in cartilage tissue engineering. J Tissue Eng Regen Med. 2007; 1:170-8.

60. Buckley CT, O'Kelly KU. Regular scaffold fabrication techniques for investigatons in tissue engineering In: P.J. Prendergast and P.E. McHugh editors, Topics in Bio-Mechanical Engineering, 2004; 147-166.

61. Lanza RP, Langer RS, Vacanti J. Biomaterials in Tissue Engineering Polymer scaffold fabrication. In: Lanza RP, Langer RS, Vacanti JP, editors. Principles of Tissue Engineering. 3rd ed. Amsterdam; Boston: Elsevier / Academic Press, 2007; 309-323.

62. Yang S, Leong KF, Du Z, Chua CK. The design of scaffolds for use in tissue engineering. Part I. Traditional factors. Tissue Eng. 2001; 7:679-89.

63. Liu W, Merrett K, Griffith M, Fagerholm P, Dravida S, Heyne B, Scaiano JC, Watsky MA, Shinozaki N, Lagali N, Munger R, Li F. Recombinant human collagen for tissue engineered corneal substitutes. Biomaterials. 2008; 29:1147-58.

64. Bostman OM. Absorbable implants for the fixation of fractures. J Bone Joint Surg 1991; 73:148-53.

65. Gelse K, Pöschl E, Aigner T. Collagens--structure, function, and biosynthesis. Adv Drug Deliv Rev. 2003; 55:1531-46.

66. Ikada Y. Scope of Tissue Engineering. In: Tissue Engineering: Fundamentals And Applications. 1st ed. Amsterdam; Boston: Academic Press/Elsevier, 2006; 1-30.

67. Lanza RP, Langer RS, Vacanti J. Introduction to Tissue Engineering. In: Lanza RP, Langer RS, Vacanti JP, editors. Principles of Tissue Engineering. 3rd ed. Amsterdam; Boston: Elsevier / Academic Press, 2007; 1-33.

68. Cen L, Liu W, Cui L, Zhang W, Cao Y. Collagen tissue engineering: development of novel biomaterials and applications. Pediatr Res. 2008; 63:492-6. doi: 10.1203/PDR.0b013e31816c5bc3.

69. Glowacki J, Mizuno S. Collagen scaffolds for tissue engineering. Biopolymers. 2008; 89:338-44.

70. Parenteau-Bareil R, Gauvin R, Berthod F. Collagen-Based Biomaterials for Tissue Engineering Applications. Materials 2010; 3:1863-1887; doi:10.3390/ma3031863.

71. Pieper JS, Oosterhof A, Dijkstra PJ, Veerkamp JH, van Kuppevelt TH. Preparation and characterization of porous crosslinked collagenous matrices containing bioavailable chondroitin sulphate. Biomaterials. 1999; 20:847-58.

72. Kinikoglu B, Rodríguez-Cabello JC, Damour O, Hasirci V. The influence of elastin-like recombinant polymer on the self-renewing potential of a 3D tissue equivalent derived from human lamina propria fibroblasts and oral epithelial cells. Biomaterials. 2011; 32:5756-64. doi:10.1016/j.biomaterials.2011.04.054.

73. Web site of Thermo-Fisher Scientific Company. Illustration retrieved from http://www.piercenet.com/browse.cfm?fldID=02030312

74. Edmonds, M. Apligraf in the treatment of neuropathic diabetic foot ulcers. Int. J. Low Extrem. Wounds 2009; 8:11–18.

75. Catledge SA, Clem WC, Shrikishen N, Chowdhury S, Stanishevsky AV, Koopman M, Vohra YK. An electrospun triphasic nanofibrous scaffold for bone tissue engineering. Biomed Mater. 2007; 2:142-50. doi: 10.1088/1748-6041/2/2/013.

76. Juncosa-Melvin N, Shearn JT, Boivin GP, Gooch C, Galloway MT, West JR, Nirmalanandhan VS, Bradica G, Butler DL. Effects of mechanical stimulation on the biomechanics and histology of stem cell-collagen sponge constructs for rabbit patellar tendon repair. Tissue Eng. 12:2291–2300.

77. Archibald SJ, Krarup C, Shefner J, Li ST, Madison RD. A collagen-based nerve guide conduit for peripheral nerve repair: An electrophysiological study of nerve regeneration in rodents and nonhuman primates. J. Comp. Neurol. 1991; 306:685–696.

78. Web site of The Medical Biochemistry. Illustration retrieved from http://themedicalbiochemistrypage.org/glycans.php

79. Lamari FN, Karamanos NK. Structure of chondroitin sulfate. In: Nicola V, editor. Chondroitin Sulfate: Structure, Role And Pharmacological Activity. Academic Press; 1st edition 2006 p.33-43

80. Park J, Lakes RS. Structure–Property Relationships of Biological Materials. In: Biomaterials: An Introduction. 3rd ed. Springer. 2007; 226-261.

81. Griffith M, Jackson WB, Lagali N, Merrett K, Li F, Fagerholm P. Artificial corneas: a regenerative medicine approach. Eye (Lond). 2009; 23:1985-9. doi: 10.1038/eye.2008.409.

82. Wang S, Liu W, Han B, Yang L. Study on a hydroxypropyl chitosan–gelatin based scaffold for corneal stroma tissue engineering. Applied Surface Science. 2009; 255:8701–5.

83. Zhong S, Teo WE, Zhu X, Beuerman R, Ramakrishna S, Yung LY. Formation of collagen-glycosaminoglycan blended nanofibrous scaffolds and their biological properties. Biomacromolecules. 2005; 6:2998-3004.

84. Paterson SM, Shadforth AMA, Brown DH, Madden PW, Chirila TV, Baker MV. The synthesis and degradation of collagenase-degradable poly(2-hydroxyethyl methacrylate)-based hydrogels and sponges for potential applications as scaffolds in tissue engineering. Materials Science and Engineering: C. 2012; 32:2536-2544.

85. Merrett K, Liu W, Mitra D, Camm KD, McLaughlin CR, Liu Y, Watsky MA, Li F, Griffith M, Fogg DE. Synthetic neoglycopolymer-recombinant human collagen hybrids as biomimetic crosslinking agents in corneal tissue engineering. Biomaterials. 2009; 30:5403-8. doi: 10.1016/j.biomaterials.2009.06.016.

86. Deng C, Li F, Hackett JM, Chaudhry SH, Toll FN, Toye B, Hodge W, Griffith M. Collagen and glycopolymer based hydrogel for potential corneal application. Acta Biomater. 2010; 6:187-94. doi: 10.1016/j.actbio.2009.07.027.

87. Kobayashi H, Kato M, Taguchi T, Ikoma T, Miyashita H, Shimmura S, Tsubota K, Tanaka J. Collagen immobilized PVA hydrogel-hydroxyapatite composites prepared by kneading methods as a material for peripheral cuff of artificial cornea. Materials Science and Engineering: C. 2004; 24:729-735.

88. Duan X, McLaughlin C, Griffith M, Sheardown H. Biofunctionalization of collagen for improved biological response: Scaffolds for corneal tissue engineering. Biomaterials 2007; 28:78-88.

89. Ponce Márquez S, Martínez VS, McIntosh Ambrose W, Wang J, Gantxegui NG, Schein O, Elisseeff J. Decellularization of bovine corneas for tissue engineering applications. Acta Biomaterialia 2009; 5:1839-1847.

90. Hashimoto Y, Funamoto S, Sasaki S, Honda T, Hattori S, Nam K, Kimura T, Mochizuki M, Fujisato T, Kobayashi H, Kishida A. Preparation and characterization of decellularized cornea using high-hydrostatic pressurization for corneal tissue engineering. Biomaterials 2010; 31:3941-3948.

91. Schwab IR, Reyes M, Isseroff RR. Successful transplantation of bioengineered tissue replacements in patients with ocular surface disease. Am J Ophthalmol 2000; 130:543-544.

92. Lawrence BD, Marchant JK, Pindrus MA, Omenetto FG, Kaplan DL. Silk film biomaterials for cornea tissue engineering. Biomaterials 2009; 30:1299-1308.

93. Liu Y, Ren L, Yao H, Wang Y. Collagen films with suitable physical properties and biocompatibility for corneal tissue engineering prepared by ion leaching technique. Mater Lett 2012;87:1-4.

94. Zorlutuna P, Builles N, Damour O, Elsheikh A, Hasirci V. Influence of keratocytes and retinal pigment epithelial cells on the mechanical properties of polyester-based tissue engineering micropatterned films. Biomaterials 2007; 28:3489-3496.

95. Liu Y, Ren L, Wang Y. Crosslinked collagen–gelatin–hyaluronic acid biomimetic film for cornea tissue engineering applications. Materials Science and Engineering: C 2013; 33:196-201.

96. Zorlutuna P, Tezcaner A, Kiyat I, Aydinli A, Hasirci V. Cornea engineering on polyester carriers. J Biomed Mater Res A. 2006; 79:104-13.

97. Orwin EJ, Hubel A. In vitro culture characteristics of corneal epithelial, endothelial, and keratocyte cells in a native collagen matrix. Tissue Eng. 2000; 6:307–319.

98. Orwin EJ, Lee S, Raub C, Icenogle T, Arman M, Cho A, Lovec R, Malone A, Haskell RC, Hoeling BM, Petersen DC. Optical coherence microscopy for the evaluation of a tissue-engineered artificial cornea. Conf Proc IEEE Eng Med Biol Soc. 2004; 2:1218-21.

99. Vrana NE, Builles N, Kocak H, Gulay P, Justin V, Malbouyres M, Ruggiero F, Damour O, Hasirci V. EDC/NHS cross-linked collagen foams as scaffolds for artificial corneal stroma. J Biomater Sci Polym Ed. 2007; 18:1527-45.

100. Wilson SE, Liu JJ, Mohan RR. Stromal-epithelial interactions in the cornea. *Prog Retin Eye Res.* 1999; 18:293–309.

101. O.Brien FJ, Harley BA, Yannas IV, Gibson LJ. The effect of pore size on cell adhesion in collagen-GAG scaffolds, Biomaterials. 2005; 26:433-441.

102. Gelinsky M. Mineralized collagen as biomaterial and matrix for bone tissue engineering. In: Meyer U, Meyer T, Handschel J, Wiesmann HP, editors. Fundamentals of tissue engineering and regenerative medicine. 1st ed. New York: Springer, 2008; 485-493.

103. Ndreu-Halili A. Collagen-based meniscus tissue engineering: design and application. PhD thesis. Middle East Technical University. Turkey. 2011.

104. Haugh MG, Murphy CM, O'Brien FJ. Novel freeze-drying methods to produce a range of collagen-glycosaminoglycan scaffolds with tailored mean pore sizes. Tissue Eng. 2010; 16:887-94.

105. Kadakia A, Keskar V, Titushkin I, Djalilian A, Gemeinhart RA, Cho M. Hybrid superporous scaffolds: an application for cornea tissue engineering. Crit Rev Biomed Eng. 2008; 36:441-71.

106. Vrana NE. Collagen-based scaffolds for cornea tissue engineering. MSc thesis. Middle East Technical University. Turkey. 2006.

107. McKegney M, Taggart I, Grant MH. The influence of crosslinking agents and diamines on the pore size, morphology and the biological stability of collagen sponges and their effect on cell penetration through the sponge matrix. J Mater Sci Mater Med. 2001; 12:833-44.

108. Ber S, Torun Köse G, Hasirci V. Bone tissue engineering on patterned collagen films: an in vitro study. Biomaterials. 2005; 26:1977-86.

109. Lu Y, Fukuda K, Li Q, Kumagai N, Nishida T. Role of nuclear factor-κB in interleukin-1-induced collagen degradation by corneal fibroblasts, Experimental Eye Research. 2006; 83:560-568.

110. Ratanavaraporn J, Rangkupan R, Jeeratawatchai H, Kanokpanont S, Damrongsakkul S. Influences of physical and chemical crosslinking techniques on electrospun type A and B gelatin fiber mats. Int J Biol Macromol. 2010; 47:431-8. doi: 10.1016/j.ijbio mac. 2010.06.008.

111. Tierney CM, Haugh MG, Liedl J, Mulcahy F, Hayes B, O'Brien FJ. The effects of collagen concentration and crosslink density on the biological, structural and mechanical properties of collagen GAG scaffolds for bone tissue engineering. J Mech Behav Biomed Mater. 2009; 2:202-9. doi: 10.1016/j.jmbbm.2008.08.007.

112. Drexler JW, Powell HM. DHT Crosslinking of Electrospun Collagen. Tissue Eng Part C Methods. 2010. [ahead of print]

113. Builles N, Bechetoille N, Justin V, André V, Barbaro V, Di Iorio E, Auxenfans C, Hulmes DJ, Damour O. Development of a hemicornea from human primary cell cultures for pharmacotoxicology testing. Cell Biol Toxicol. 2007; 23:279-92.

114. Ma L, Gao C, Mao Z, Shen J, Hu X, Han C. Thermal dehydration treatment and glutaraldehyde cross linking to increase the biostability of collagen-chitosanporous scaffolds used as dermal equivalent. J Biomater Sci Polym Ed. 2003; 14:861-74.

115. Recum AV, Shannon CE, Cannon CE, Long KJ, Van Kooten T, Meyle J. Surface Roughness, Porosity, and Texture as Modifiers of Cellular Adhesion. Tissue Engineering. 1996; 2: 241-253. doi:10.1089/ten.1996.2.241.

116. Bahçecioğlu G. Poly(L-lactic acid) (PLLA)-based meniscus tissue engineering.. MSc thesis. Middle East Technical University. Turkey. 2011.

117. Zorlutuna P. Cornea Engineering on biodegradable polyesters. Msc thesis. Middle East Technical University. Turkey. 2011.

118. Builles N, Justin V, Andre´ V, Burillon C, Damour O. Reconstructed corneas: effect of three-dimensional culture, epithelium, and tetracycline hydrochloride on newly synthesized extracellular matrix. Cornea. 2007; 26:1239–1248.

119. Orwin EJ, Borene ML, Hubel A. Biomechanical and optical characteristics of a corneal stromal equivalent. J Biomech Eng. 2003; 125:439–444.

120. Chen J, Li Q, Xu J, Huang Y, Ding Y, Deng H, Zhao S, Chen R. Study on biocompatibility of complexes of collagen-chitosan-sodium hyaluronate and cornea. Artif Organs. 2005; 29:104–113.

121. Liu Y, Gan L, Carlsson DJ, Fagerholm P, Lagali N, Watsky MA, Munger R, Hodge WG, Priest D, Griffith M. A simple, cross-linked collagen tissue substitute for corneal implantation. Invest Ophthalmol Vis Sci. 2006; 47:1869-75.

122. Meek KM, Leonard DW, Connon CJ, Dennis S, Khan S. Transparency, swelling and scarring in the corneal stroma. Eye (Lond). 2003;17:927-36.
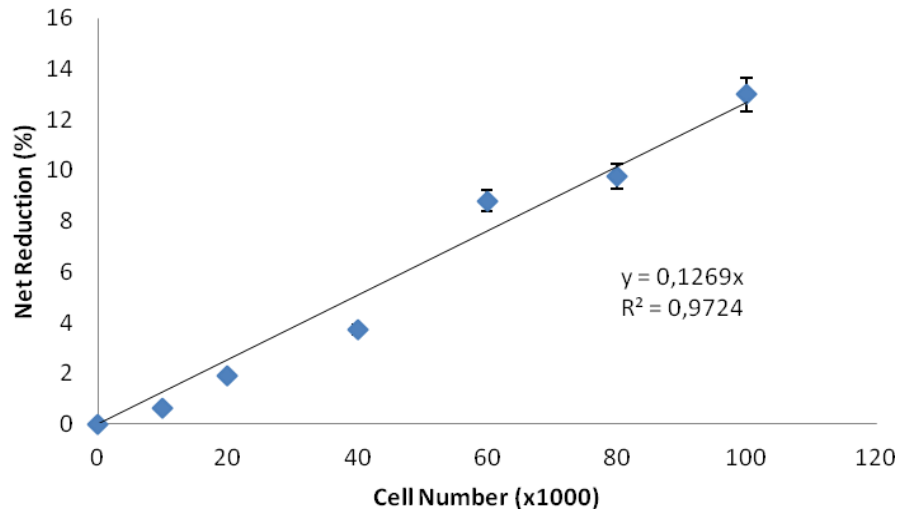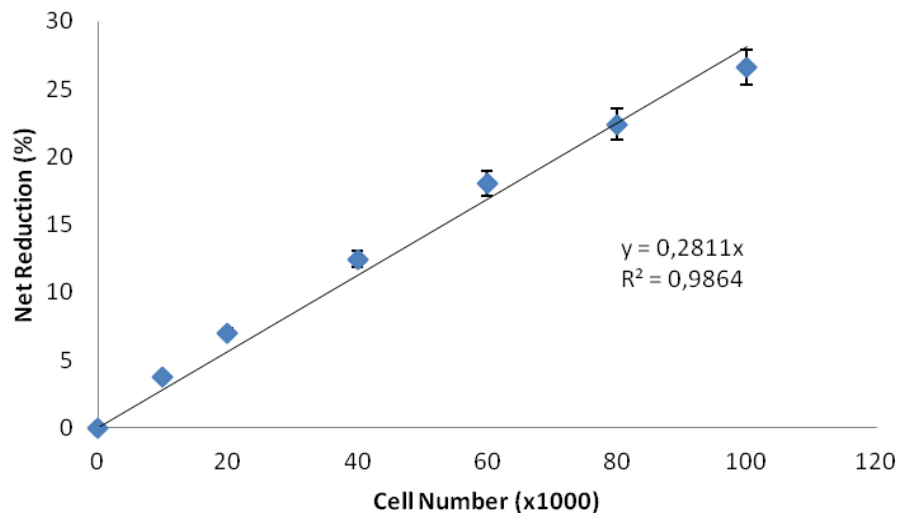
APPENDIX A

LIGHT TRANSMITTANCE OF NATIVE CORNEA
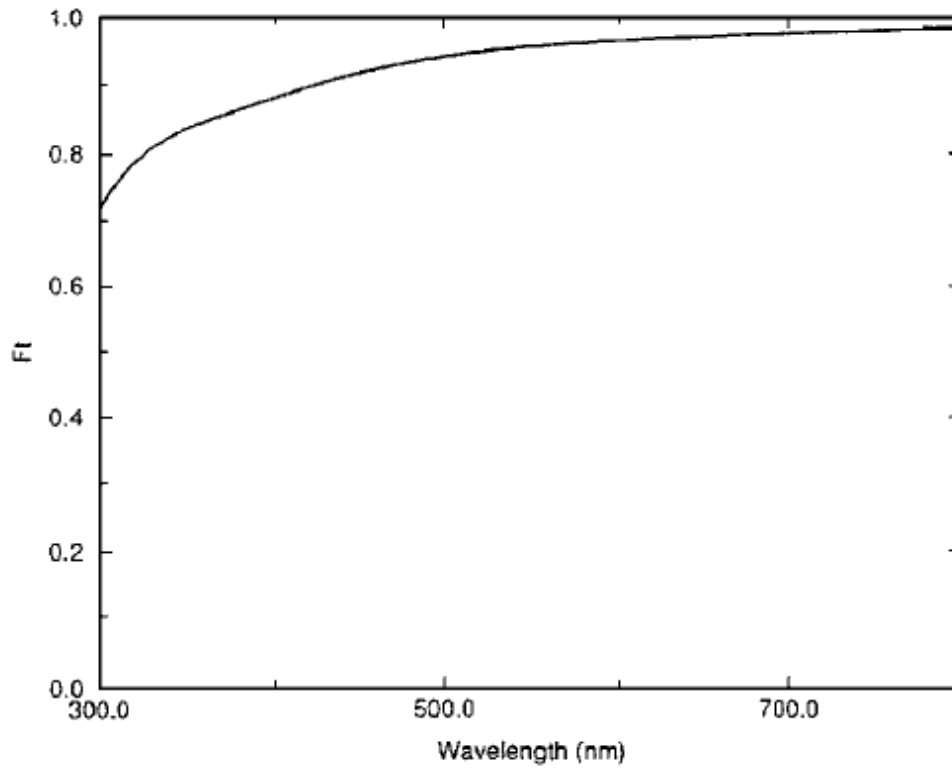
Figure A.1. Light transmittance of native cornea. The summation of scattered fields method was used to predict transmission (Ft) as a function of wavelength in the human cornea. [122]

ALAMAR BLUE CALIBRATION CURVES

Figure B.1. Alamar blue assay calibration curve for isolated human corneal keratocytes.

Figure B.2. Alamar blue assay calibration curve for D407 retinal pigment epithelial cells